NASA Technical Memorandum 82722

Nitridation of Silicon

Nancy J. Shaw
Lewis Research Center
Cleveland, Ohio

October 1981

NASA

1. Report No.	2. Government Accession No.	3. Recipient's Catalog No
NASA TM-82722		

4. Title and Subtitle	5. Report Date
NITRIDATION OF SILICON	October 1981
	6. Performing Organization Code 505-33-12

7. Author(s)	8. Performing Organization Report No.
Nancy J. Shaw	E-921
	10. Work Unit No.

9. Performing Organization Name and Address	11. Contract or Grant No.
National Aeronautics and Space Administration Lewis Research Center Cleveland, Ohio 44135	
	13. Type of Report and Period Covered
12. Sponsoring Agency Name and Address	Technical Memorandum
National Aeronautics and Space Administration Washington, D.C. 20546	14. Sponsoring Agency Code

15. Supplementary Notes

Report was submitted as a thesis in partial fulfillment of the requirements for the degree Master of Science to Case Western Reserve University, Cleveland, Ohio in August 1981.

16. Abstract

Silicon powders with three levels of impurities, principally Fe, were sintered in He or H_2. Non-densifying mechanisms of material transport were dominant in all cases. High purity Si showed coarsening in He while particle growth was suppressed in H_2. Lower purity powder coarsened in both He and H_2. The same three Si powders and Si {111} single crystal wafers were nitrided in both N_2 and N_2/H_2 atmospheres. H_2 increased the degree of nitridation of all three powders and the α/β ratio of the lower purity powder. Si_3N_4 whiskers and open channels through the surface nitride layer were observed in the presence of Fe, correlating with the nitridation-enhancing effects of Fe. Thermodynamic calculations showed that when SiO_2 is present on the Si, addition of H_2 to the nitriding atmosphere decreases the amount of SiO_2 and increases the partial pressure of Si-containing vapor species, e.g. Si and SiO. Large amounts of NH_3 and SiH_4 were also predicted to form.

17. Key Words (Suggested by Author(s))	18. Distribution Statement
Reaction bonded silicon nitride; Nitridation; Effects of H_2 and Fe on nitridation; Sintering of Si; Si single crystal nitridation	Unclassified - unlimited STAR Category 27

19. Security Classif. (of this report)	20. Security Classif. (of this page)	21. No. of Pages	22. Price*
Unclassified	Unclassified		

* For sale by the National Technical Information Service, Springfield, Virginia 22161

ATTENTION

PORTIONS OF THIS REPORT ARE NOT LEGIBLE.
HOWEVER, IT IS THE BEST REPRODUCTION
AVAILABLE FROM THE COPY SENT TO NTIS.

TABLE OF CONTENTS

CHAPTER		PAGE
	Summary	ii
I.	Introduction	1
II.	Literature Survey	3
	Structure	3
	Formation and Morphology	6
	Nitridation	9
	Hydrogen	10
	Iron	13
III.	Experimental Procedure	19
	Thermodynamic Data and Calculations	21
	Sintering and Nitridation	24
IV.	Results and Discussion	32
	Thermodynamics	32
	Sintering of Si Powder Compacts	50
	Nitridation of Si Powder Compacts	62
	Nitridation of Si Single Crystal Wafers	84
V.	Conclusion	98
VI.	Suggestions for Future Work	101
VII.	References	102

NITRIDATION OF SILICON

by Nancy Jean Shaw

National Aeronautics and Space Administration
Lewis Research Center
Cleveland, Ohio

SUMMARY

Silicon powders with three levels of impurities, principally Fe, were sintered in He or H_2. Non-densifying mechanisms of material transport were dominant in all cases. High purity Si showed coarsening in He while particle growth was suppressed in H_2. Lower purity powder coarsened in both He and H_2.

The same three Si powders and Si {111} single crystal wafers were nitrided in both N_2 and N_2/H_2 atmospheres. H_2 increased the degree of nitridation of all three powders and the α/β ratio of the lower purity powder. Si_3N_4 whiskers and open channels through the surface nitride layer were observed in the presence of Fe, correlating with the nitridation-enhancing effects of Fe.

Thermodynamic calculations showed that when SiO_2 is present on the Si, addition of H_2 to the nitriding atmosphere decreases the amount of SiO_2 and increases the partial pressure of Si-containing vapor species, e.g. Si and SiO. Large amounts of NH_3 and SiH_4 were also predicted to form.

I. INTRODUCTION

The formation of Si_3N_4 is a simple process. Silicon is heated in the presence of $N_2(g)$, which reacts according to

$$3Si + 2N_2 = Si_3N_4 \qquad (1)$$

In actuality, the reaction is not that simple. First of all, the Si is covered by a layer of SiO_2 that must be removed or at least disrupted before the N_2 can reach the Si. Most Si powder that is used in the production of reaction-bonded Si_3N_4 (RBSN) contains impurities such as Fe, Al, C, Ca, Ni, Zr, O, etc. Some of these, particularly Fe, have dramatic effects on the nitridation process. Minor amounts of impurities, such as H_2O and O_2 in the N_2, are also of concern. Gaseous species may also be evolved from the furnace hardware. Other gases such as H_2 and He may be added because they appear to favorably affect nitridation.

Over the past 15-20 years, much effort has gone into understanding the process of silicon nitridation. However, the experiments have seldom been of a type that could really determine the mechanisms of nitridation. Due to the apparent critical importance of many minor constituents and processing variables to the final result, it is not always clear that the changing conditions being observed were really responsible for the changes in the product.

The aim of this study was to understand the effects of H_2 and Fe on the final microstructure and phase composition of RBSN.

The study was done in four parts:

1) An analysis of the effects of H_2 by means of a computer program that uses thermodynamic data to determine complex chemical equilibria,
2) A study of the microstructural development of a Si powder compact in the presence of H_2 and/or Fe during sintering to determine effects that occur during presintering or heating to nitridation temperature;
3) A study of the final RBSN microstructure and ratio of α-Si_3N_4 to β-Si_3N_4 (α/β ratio) as a function of the presence or absence of H_2 and Fe; and
4) Nitridation of {111} wafers of Si single crystals to study the formation of Si_3N_4 at the Si surface and to aid in differentiating impurity effects from morphology effects.

II. LITERATURE SURVEY

Structure

Si_3N_4 has two crystal modifications designated α and β. Both are hexagonal and made up of Si - N tetrahedra.

β-Si_3N_4 is made up of identical layers of Si - N tetrahedra. Its structure (Figure 1) has been determined unambiguously (Hardie and Jack 1957; Ruddlesden and Popper 1958; Forgeng and Decker 1958). It belongs to space group $P6_3/m$, No. 176 with 6 Si in 6 (h) at (x = 0.173, y = -0.231, z = 0.250), 6 N in 6 (h) at (0.332, 0.031, 0.250) and 2 N in 2 (c) at (0.333, 0.667, 0.250) (Wild, Grievison and Jack 1972).

The structure of α-Si_3N_4 (Figure 2) is made up of two layers of tetrahedra. The first layer is like that of β. The second is a mirror image of the first (Thompson and Pratt 1967). It has been suggested that α-Si_3N_4 is actually an oxynitride containing ~ 1.5 weight percent oxygen and having a formula of $Si_{11.5}N_{15}O_{0.5}$ (Wild et al. 1972). It was later shown (Priest, Burns, Priest and Skaar 1973) that α-Si_3N_4 could be prepared containing much less oxygen than needed for such a structure. Kohatsu and McCauley (1974) have also concluded from x-ray diffractometer analysis of α-Si_3N_4 single crystals that α does not contain oxygen in the structure. The space group is $P3_1C$,

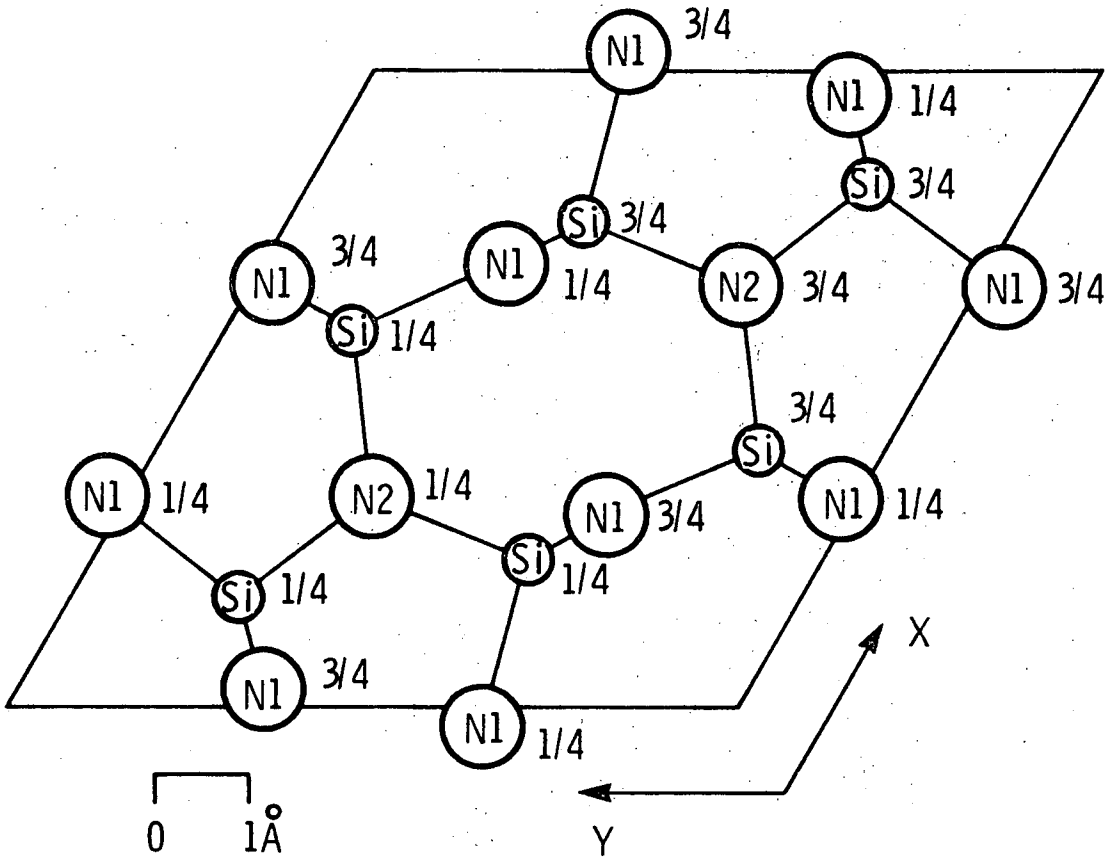

Figure 1. - The structure of β-Si_3N_4.
(Cartz and Jorgensen, 1981)

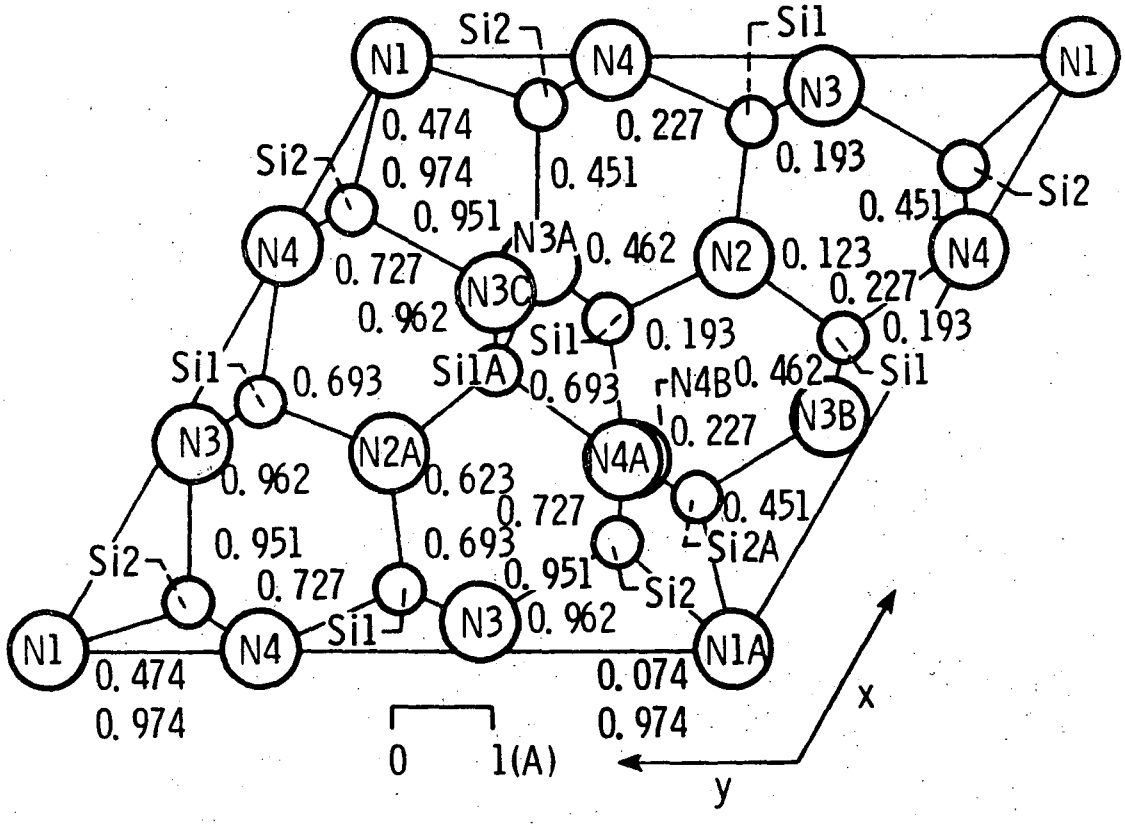

Figure 2. - Structure of α-Si_3N_4.
(Cartz and Jorgensen, 1981)

No. 159. Evans and Sharp (1971) have determined the atom locations to be 6 Si in 6 (c) at (0.0724, 0.5013, 0.6462), 6 Si in 6 (c) at (0.2554, 0.1673, 0.4509), 6 N in 6 (c) at (0.6331, 0.5936, 0.4001), 6 N in 6 (c) at (0.3210, 0.3103, 0.6701), 2 N in 2 (b) at (0.3333, 0.6667, 0.615) and 2 N in 2 (a) at (0.000, 0.000, 0.385). Slightly different positions are indicated in Figure 2.

It is generally believed that α-Si_3N_4 is a low temperature form and β a high temperature form. However, both forms usually occur at any nitriding temperature. It has been suggested (Grieveson, Jack and Wild 1968) that α is the "high oxygen potential" and β the "low oxygen potential" form. Another suggestion (Blegen 1975) is that β is the stable modification at all temperatures and α is metastable, witn formation of each polymorph being determined by the kinetics of the mechanism involved. Chemical kinetics and mechanistic studies of Si_3N_4 formation have not been reported.

Formation and Morphology

The mechanisms of formation of Si_3N_4 and resultant morphologies are still open to question. Before looking at the specifics of the literature on the subject, we should note the prevailing assumptions.

It is generally accepted that α-Si_3N_4 forms by the vapor phase reaction of a Si vapor species and N_2, resulting in high aspect ratio (length: diameter) whiskers, but whether that vapor species is Si (Dawson and Moulson 1978) or SiO (Lindley, Elias, Jones, and Pitman 1979) is still in dispute. In RBSN, these whiskers form a very fine "mat" in the space between the original Si particles. β-Si_3N_4 is believed to form either by direct nitridation of solid Si or by nucleation within and precipitation from a liquid phase (usually believed to be $FeSi_2$) in contact with N_2 (Lindley et al., 1979; Moulson 1979). β-Si_3N_4 forms as relatively large particles at the site of the original Si particles and in the Fe-rich regions surrounding large pores (Dawson, Arundale and Moulson 1977).

The literature contains many Scanning Electron Microscopy (SEM) or polished section photomicrographs of the type shown in Figure 3. The fine areas are usually identified as α and the larger dense regions at β, but without any type of analysis that could confirm that this is indeed the case. In most cases conclusions are then drawn, based on the assumed microstructure, about the effects of the processing variables being considered.

A few percent of H_2 is usually added to the N_2. It is supposed to help form a finer, more uniform microstructure (Mangels 1975) by lowering the partial pressure of O_2 so that more SiO will

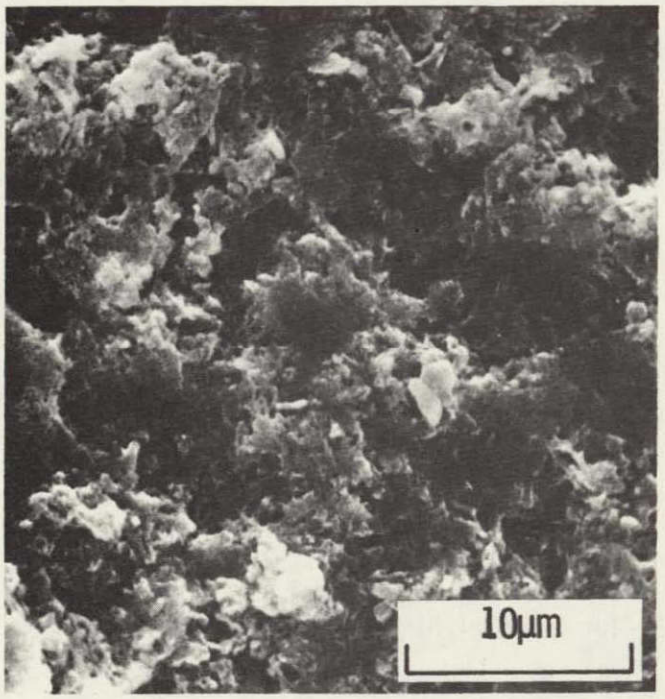

FIGURE 3

SEM micrograph of Si_3N_4 formed by reaction of high purity Si powder and N_2 at 1375°C.

TABLE 2

CHARACTERIZATION OF SILICON POWDERS

	Commercial-grade	High purity
	ppm	ppm
Al	0.1 percent	-
C	0.32 percent	0.34 percent
Ca	200	-
Cr	410	-
Cu	80	-
Fe	0.6 percent	-
Mg	110	-
Mn	330	-
N	60	-
Ni	150	40
O	1.28 percent	0.51 percent
Sr	-	5
Ti	150	-
V	180	-
Zr	110	-
Si	balance	balance
BET Surf. area, m^2/g	7.4	7.99

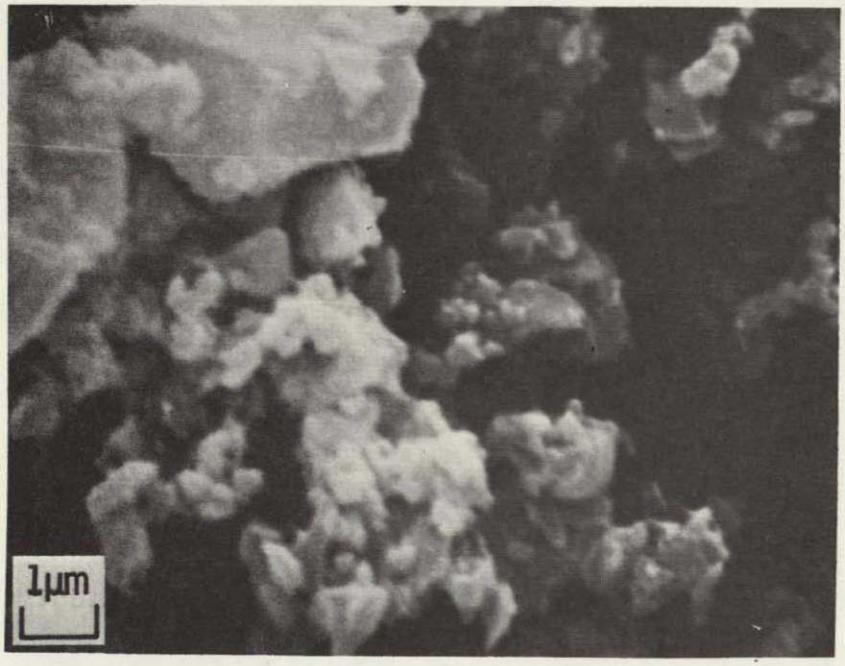

Figure 4. SEM micrograph of milled Si powder

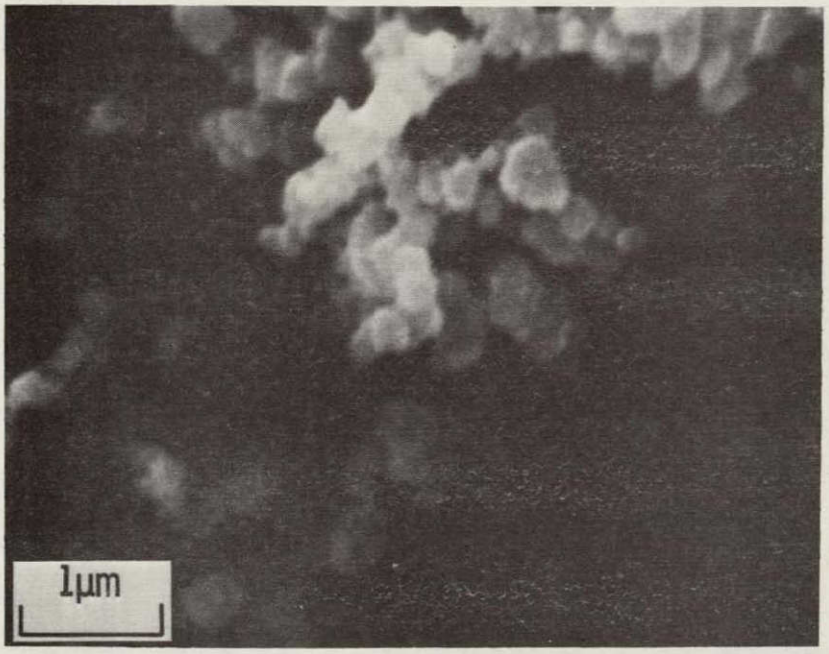

Figure 5. SEM micrograph of high purity Si powder

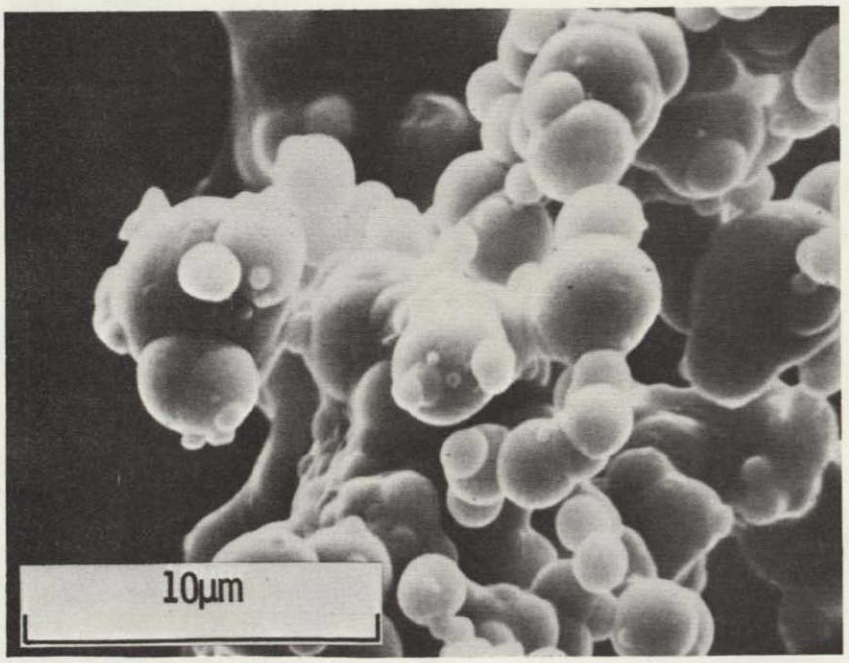

Figure 6. SEM micrograph of high purity Fe powder

The crystallographic orientation of the wafer faces was {111}.

All sintering and nitridation was done in furnaces with high density Al_2O_3 tubes and external SiC heating elements. Samples were placed on RBSN setters in high density Al_2O_3 boats with the specimens above the sides of the tray, completely exposed to the gas flow. The ends of the tube were sealed with stainless steel covers and silicone rubber gaskets. Gas inlet and outlet and thermocouple insertion was through these end seals. All piping for the gas supply was stainless steel. Internal heat shields were mullite in the sintering furnace and high density Al_2O_3 in the nitriding furnace.

The nitriding furnace was supplied with oxygen-free N_2 and custom-grade N_2/4 percent H_2 cylinder gas used without further treatment. Gas flow was < 20 ml $min.^{-1}$ Sintering was for 5h at 1375^{o}C and nitriding for 4h, under the conditions listed in Table 3. The specimen was heated to the nitriding temperature in the desired atmosphere and then nitrided 4h without removing it from the hot zone of the furnace in the same gas, or the desired N_2 or N_2/H_2 after heating in He.

X-ray diffraction analysis of nitrided samples was done using Kα Cu radiation on powder abraded with a diamond burr from a cross-sectional surface of the wafer. Determination of the amounts

TABLE 3

NITRIDATION CONDITIONS

HEAT/COOL ATM	TEMPERATURE
N_2/H_2	1200°C
He	1200°C
N_2/H_2	1375°C
He	1375°C

N_2/H_2 was the same as that used for the nitridation:

N_2/H_2 = N_2

= N_2/1 Percent H_2

= N_2/4 Percent H_2

of α-and β-Si_3N_4 and retained Si was done using the method developed by Gazzara and Messier (1977).

Scanning electron microscope (SEM) examination of all specimens was made on fracture surfaces.

IV. RESULTS AND DISCUSSION

Thermodynamics

$SiO_2/N_2/H_2$ Systems

If it is assumed that each silicon particle is covered by an impervious layer of SiO_2 prior to nitridation, the system can then be considered to consist of only silica, nitrogen and hydrogen. The initial compositions of the systems investigated are listed in Table 4. The silica in a real system represents a relatively small fraction of the total amount of Si plus SiO_2. Therefore, the amount of nitriding gas was taken to be 100 times larger than what will be used in the $Si/N_2/H_2/O_2$ systems.

There are two condensed species that appear in the $SiO_2/N_2/H_2$ systems; SiO_2 and Si_3N_4. Figure 7 is a plot of the mole fraction of solid silica vs. temperature from 1000^oK to 2000^oK with H_2 as a parameter. The usual temperature range for nitridation is indicated for reference. As can be seen in Figure 7a, less than 15 percent of the $SiO_2(s)$ initially present is removed by 10 percent H_2 at the highest nitriding temperature. At the low temperature end of the nitriding region, the H_2-enhanced reduction in the amount of $SiO_2(s)$ is very slight.

TABLE 4. - INITIAL COMPOSITIONS OF $SiO_2/N_2/H_2$ SYSTEMS

System designation	0 Percent H_2	4 Percent H_2	10 Percent H_2	100 Percent H_2
N_2, mole	200	192	180	---
H_2, mole	---	8	20	200
SiO_2, mole	0.2	0.2	0.2	0.2

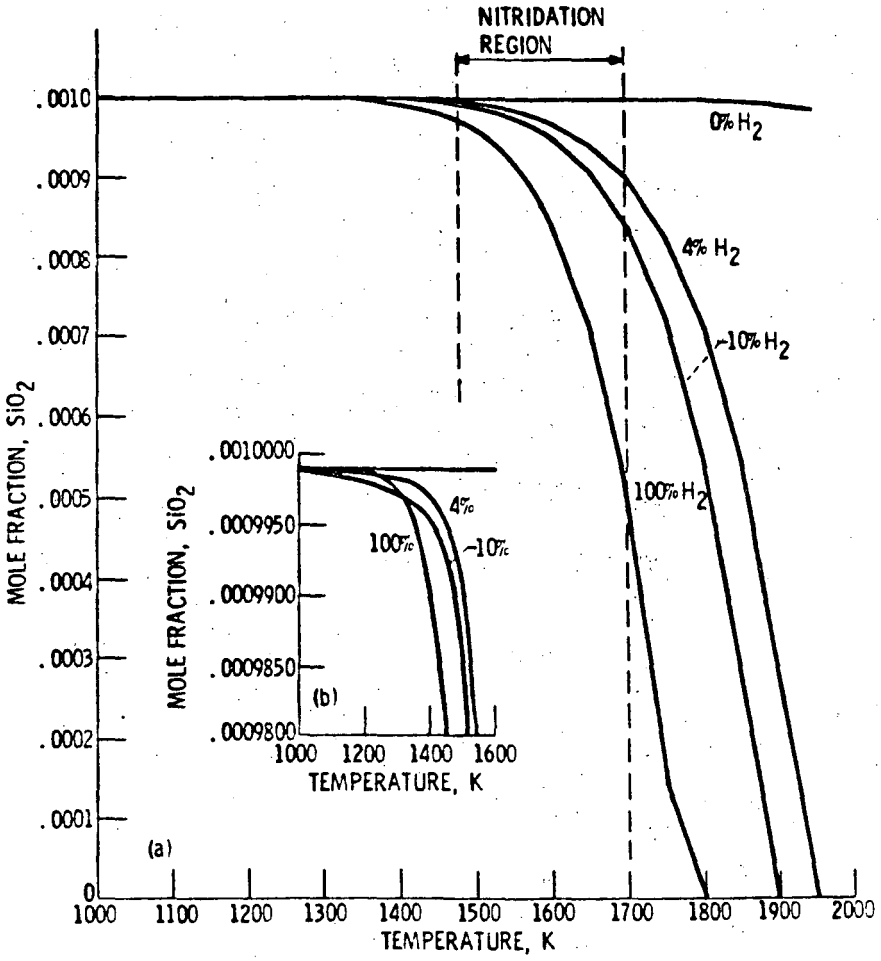

Figure 7. - (a) Effect of H_2 in decreasing mole fraction of SiO_2(s) formed at equilibrium in $SiO_2/N_2/H_2$ systems. (b) Enlarged portion of 7(a) to show effect of H_2 in reducing the temperature at which amount of SiO_2 is reduced.

At temperatures higher than normal nitriding temperatures, the amount of $SiO_2(s)$ is reduced drastically when H_2 is present. Although the difference in amount of $SiO_2(s)$ formed as shown in Figure 7b is extremely slight, it is of interest to note that 4 percent and 10 percent H_2 additions to N_2 result in less $SiO_2(s)$ at low temperatures than does pure H_2 due to the simultaneous formation of $Si_3N_4(s)$ when H_2 is present.

It seems quite likely that hydrogen may promote the removal of enough of the silica to induce flaws in the silica film. In the absence of H_2, there is essentially no reduction in the amount of silica even to temperatures as high as its melting point, and some other mechanism such as that involving iron suggested by Moulson (1979) would be required to disrupt the silica layer. Si_3N_4 does not form at any temperature in the interval 1000^{o} - $2000^{o}K$ in a system composed of only SiO_2 and N_2. Addition of H_2 to the system allows formation of Si_3N_4. Although the amount formed is small, as can be seen in Figure 8, increasing the H_2 content from 4 percent to 10 percent has an effect on both the amount present, and the maximum temperature at which it is stable. However, in neither of these cases is Si_3N_4 formed in the usual nitridation temperature region.

Many vapor species form in these systems. Those considered to be of particular interest will be discussed with reference to

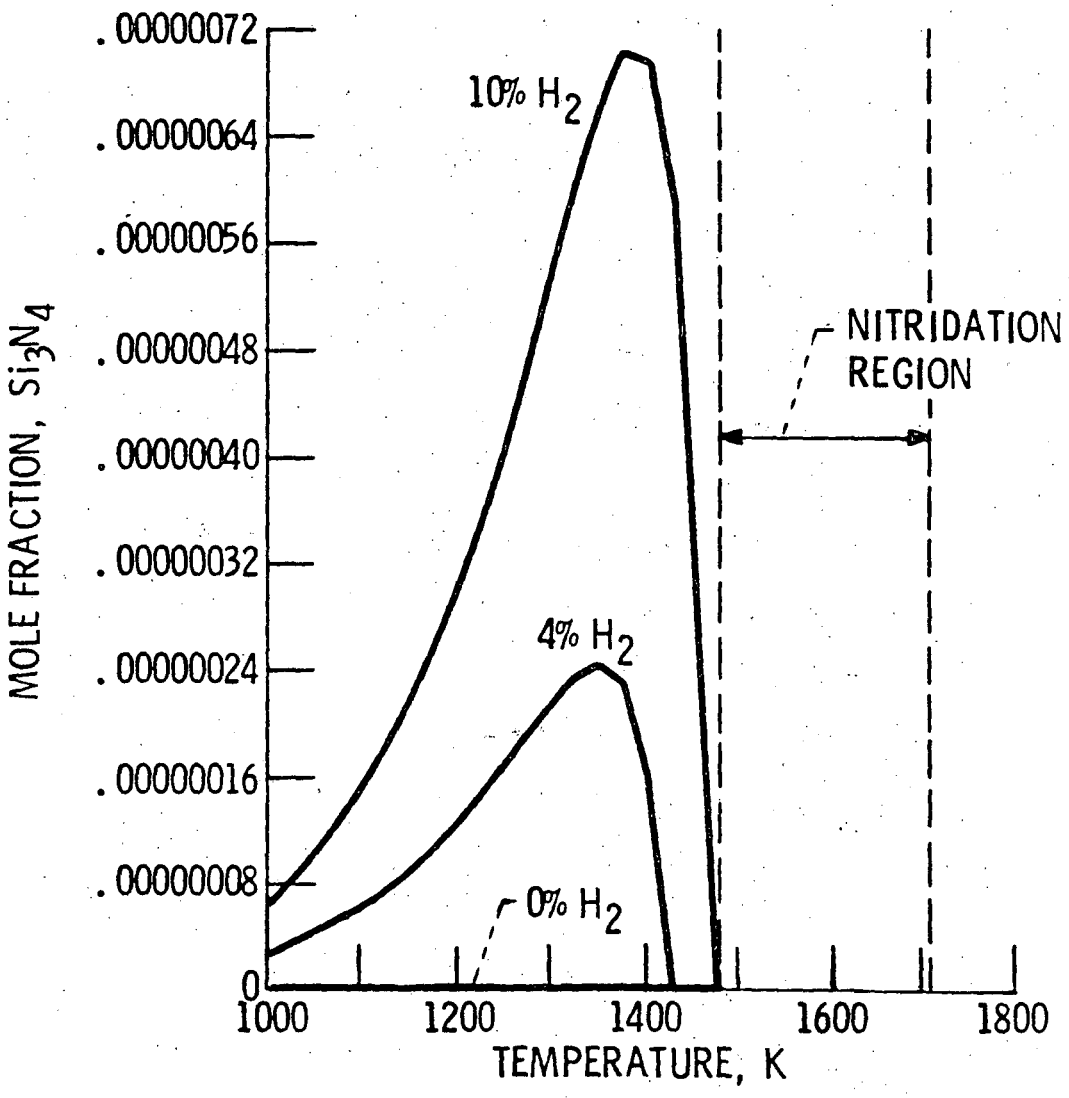

Figure 8. - Mole fraction of Si_3N_4(s) formed in $SiO_2/N_2/H_2$ systems. No Si_3N_4 is formed in pure N_2.

Figures 9 - 14. Each of these figures is a plot of the partial pressure of a vapor species against temperature. Each shows calculated values from the two sets of systems ($SiO_2/N_2/H_2$ and $Si/N_2/H_2/O_2$) considered. The low temperature region on the left contains the plots for the $SiO_2/N_2/H_2$ systems. These plots will be discussed first. The high temperature region on the right, which includes the nitridation region, contains the plots of the systems composed of Si, N_2, H_2 and O_2 to be discussed later. Within the nitridation region, both sets of curves are shown to contrast the behavior of the two sets of systems.

As discussed earlier, most workers in the field have predicted that one of the most significant effects of the addition of H_2 would be an increase in the concentration (partial pressure) of SiO. As can be seen in Figure 9, that is indeed the case. The p_{SiO} is increased 3 to 5 orders of magnitude by the addition of 4 or 10 percent H_2. The higher partial pressure for 10 percent H_2 above ~ 1450^{o}K reflects the greater decrease in the amount of SiO_2(s) present in the system.

The other major effect of H_2 is expected to be a decrease in the P_{O_2}. This effect does occur and can be seen in Figure 10. At 1475^{o}K, the log p_{O_2} is decreased from -12.5 to -20 by addition of 4 percent H_2.

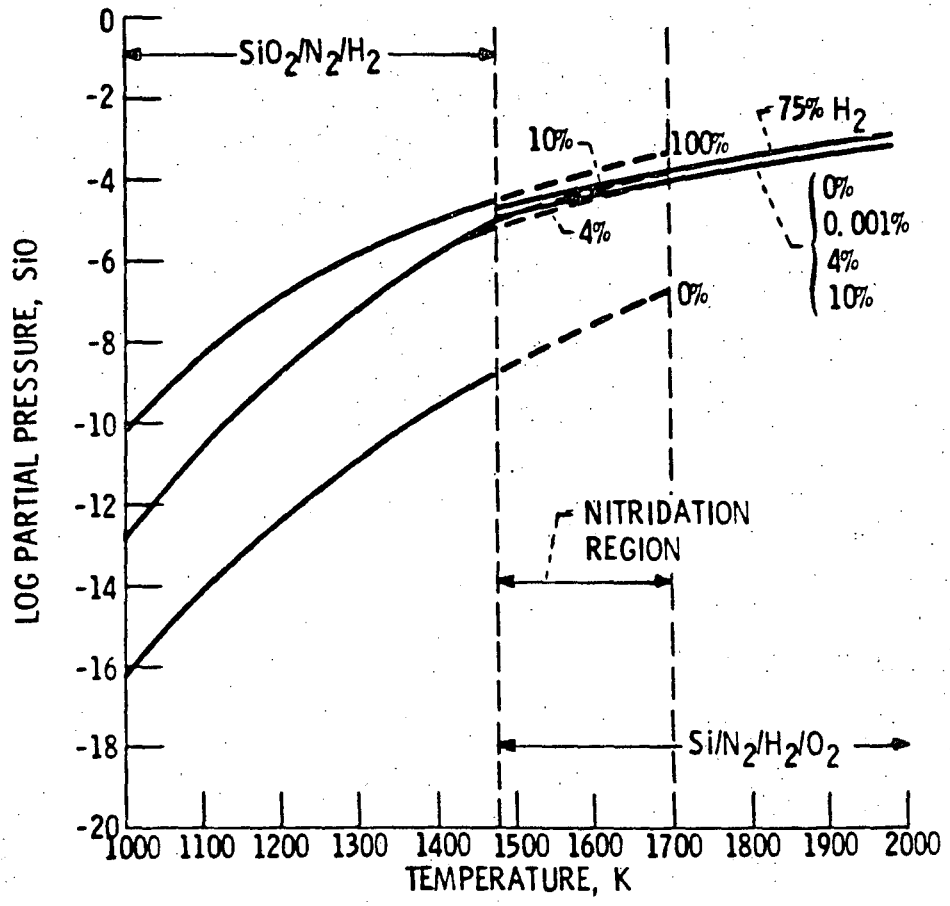

Figure 9. - Equilibrium partial pressure of SiO is strongly affected by H_2 concentration in $SiO_2/N_2/H_2$ systems, but not in $Si/N_2/H_2/O_2$ systems.

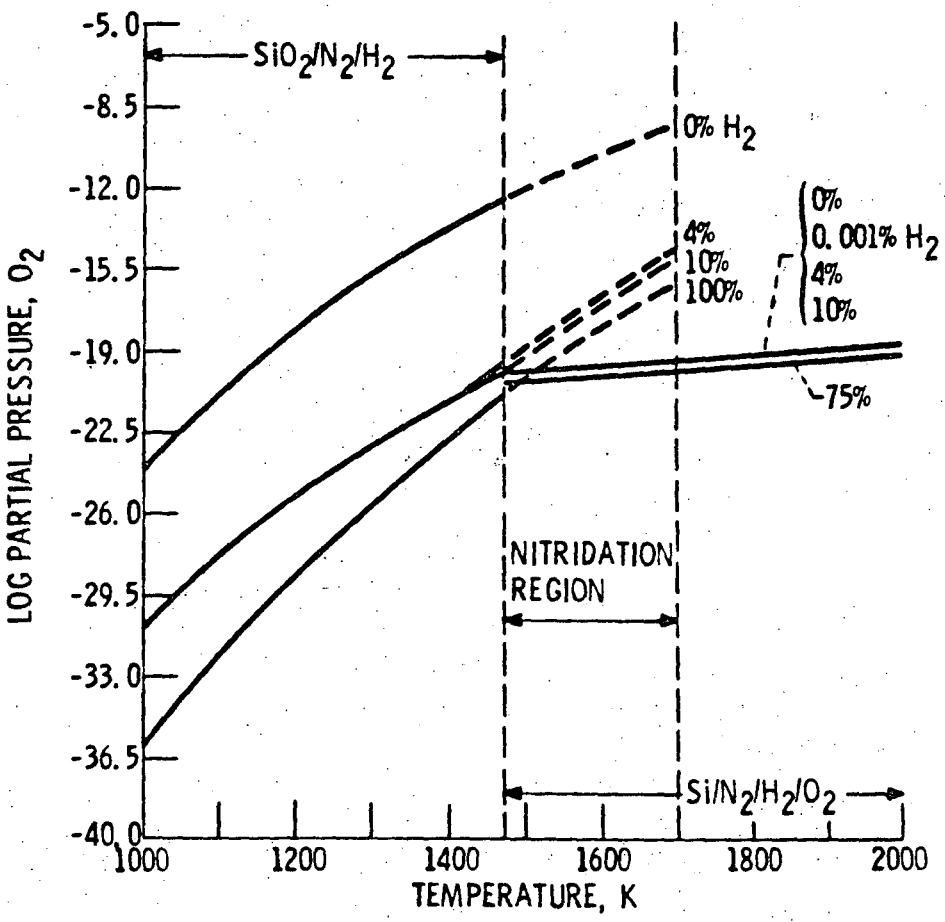

Figure 10. - Effect of H_2 content in reducing equilibrium partial pressure of O_2 in $SiO_2/N_2/H_2$ systems on left. Little effect of H_2 is seen in $Si/N_2/H_2/O_2$ systems on right.

The effect of H_2 on the concentration of Si (Figure 11) is much the same as for SiO; however, it should be noted that p_{Si} is from 8 to 10 orders of magnitude lower than p_{SiO}. This large disparity in concentrations, if it persisted away from equilibrium, could favor SiO(g) over Si(g) as a source of Si_3N_4.

Moulson (1979) has suggested the importance of H_2O in the formation of silicon nitride. Our calculated partial pressures of $H_2O(g)$ are shown in Figure 12. At 1475^{o}K, p_{H_2O} is greater than that of any vapor species except N_2 and H_2. It is interesting that at very low temperatures, less $H_2O(g)$ forms in an atmosphere initially 100 percent H_2 than in one containing 4 percent or 10 percent H_2.

Most of the other vapor species listed in Table 2 are also present although most are in amounts that appear to be quite insignificant. However, any of them, particularly the simpler molecules, may be of significance in the actual nitridation mechanism due to kinetic effects. None of these species appear in the simple reactions (e.g. Equations 1-8) usually considered relevant to the nitridation of Si.

Two gaseous species not previously reported that may be of importance are NH_3 and SiH_4 (Figure 13 and 14, respectively). The concentrations of both are, of course, dependent on the concentration of H_2. At the lowest temperatures, the partial

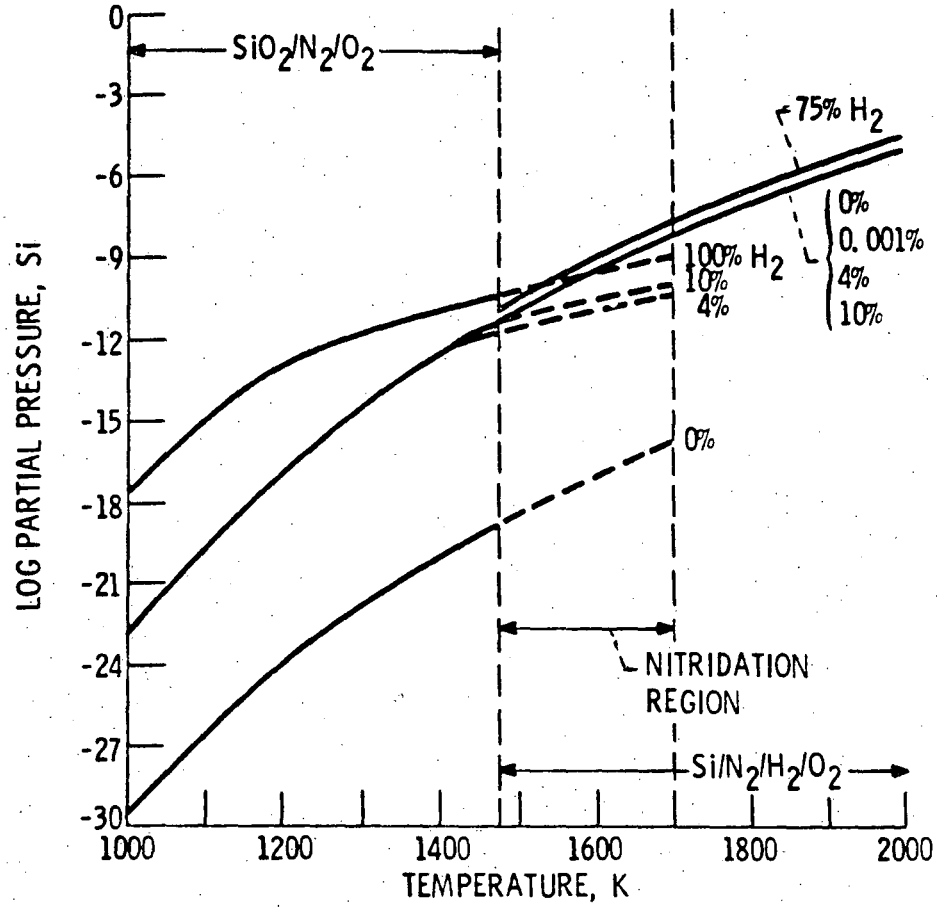

Figure 11. - H_2 concentration strongly affects partial pressure of Si in $SiO_2/N_2/H_2$ systems, but not in $Si/N_2/H_2$ systems.

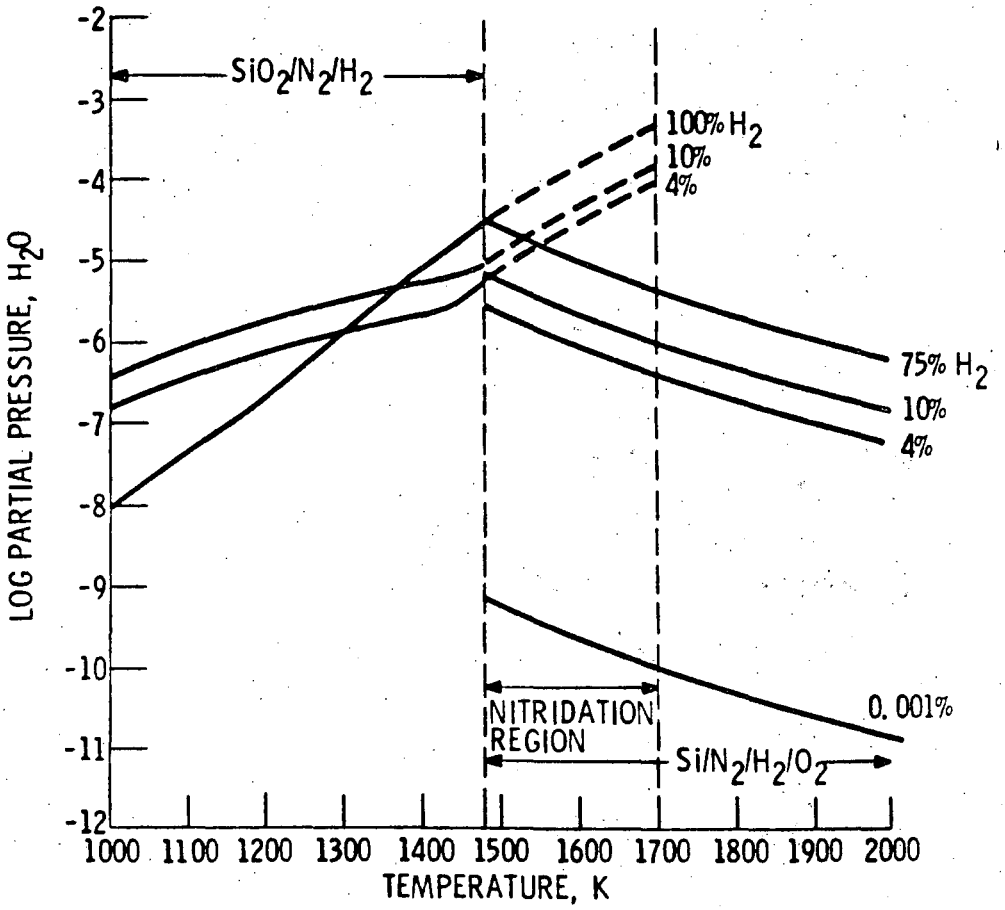

Figure 12. - Partial pressure of H_2O is a function of H_2 content in both $SiO_2/N_2/H_2$ and $SiN_2/H_2/O_2$ systems.

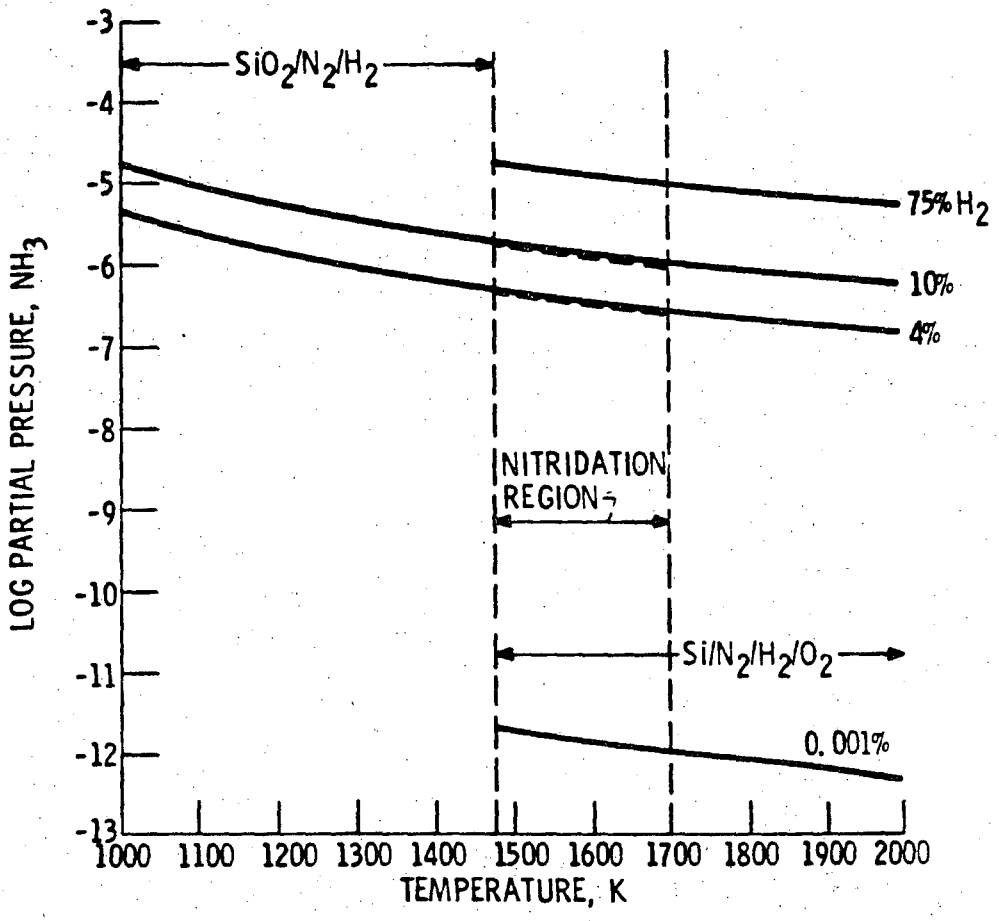

Figure 13. - Equilibrium partial pressure of NH_3 increases with increasing H_2 content and is the same for both $SiO_2/N_2/H_2$ and $Si/N_2/H_2/O_2$ systems.

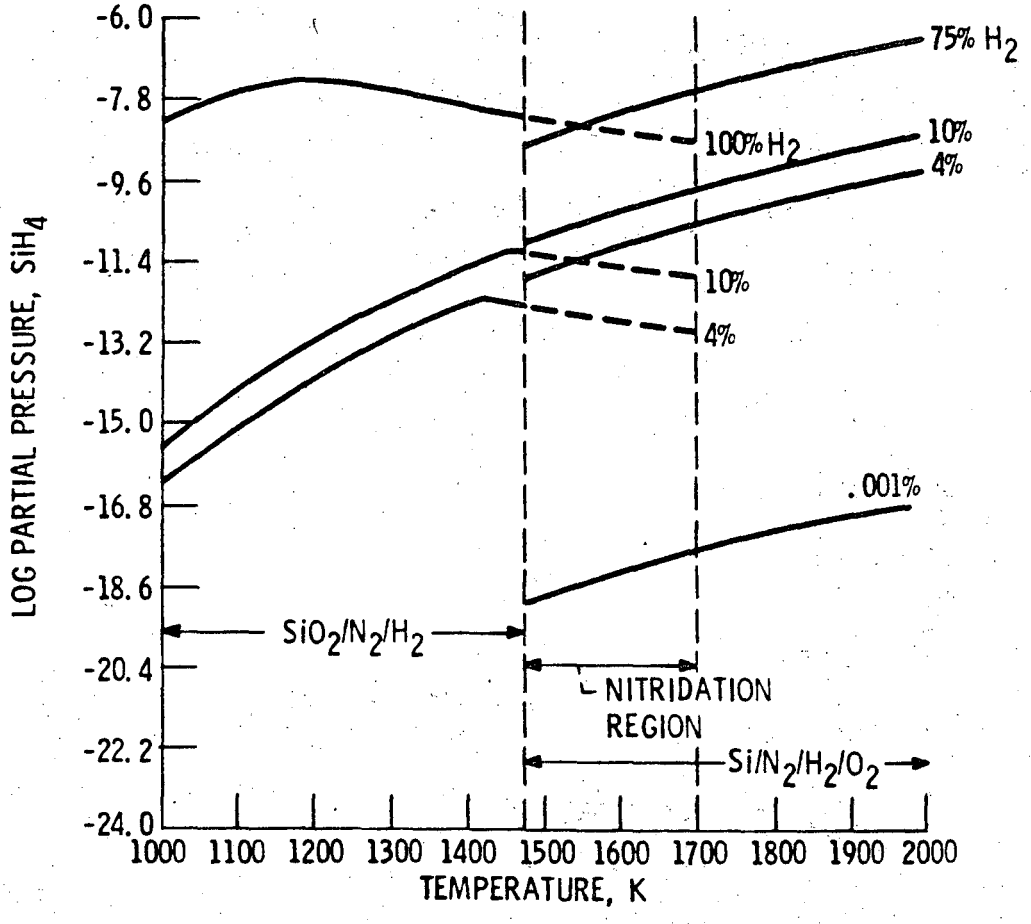

Figure 14. - Increasing amounts of H_2 increase partial pressure of SiH_4 in $SiO_2/N_2/H_2$ and $Si/N_2/H_2/O_2$ systems.

pressure of NH_3 is higher than that of any other gas present except N_2 and H_2. At 1475°K, its partial pressure is also exceeded slightly by those of H, H_2O and SiO. The partial pressure of SiH_4, as shown in Figure 14, is much less than that of NH_3, but is among the higher ones in the nitridation temperature range. The combining of NH_3 and SiH_4 is one of the methods used to form chemically vapor deposited (CVD) Si_3N_4 which forms in either the α-crystalline form or in an amorphous form. This process may make an important contribution to the formation of α-Si_3N_4 during nitridation.

On the basis of the preceeding figures, it is evident that the addition of hydrogen to the nitriding atmosphere significantly affects the concentrations of phases present at equilibrium during the low temperature portion of the nitriding cycle when an impervious layer of SiO_2 surrounds each Si particle. The H_2 enhances removal of the SiO_2, decreases p_{O_2}, increases p_{SiO}, p_{Si}, p_{H_2O}, p_{NH_3}, p_{SiH_4} and allows formation of a small amount of Si_3N_4.

$Si/N_2/H_2/O_2$

The calculations have shown (Figure 7) that through the nitridation temperature region neither increasing hydrogen content nor increasing temperature will result in complete removal of the silica layer surrounding each silicon particle, although it must be

disrupted by some means to allow nitridation of the underlying Si to occur. In any case, once the SiO_2(s) layer is disrupted exposing the silicon, the system then becomes one composed largely of silicon, nitrogen and hydrogen with small amounts of oxygen. Table 5 lists the initial compositions of the $Si/N_2/H_2/O_2$ systems studied. The amount of oxygen was chosen to reflect approximately the amount contained in a film of SiO_2 covering the Si plus two ppm in the gas. However, this system contains much less oxygen than the $SiO_2/N_2/H_2$ system because of the additional Si now being considered.

There are three solid species that form in these systems: Si_3N_4, Si_2N_2O, and SiO_2. Si_3N_4 is thermodynamically stable at all temperatures in the range of 1000^{o} - 2000^{o}K along with either SiO_2 or Si_2N_2O. The amount formed is essentially not a function of either hydrogen content or temperature.

SiO_2 is stable at the lower temperatures and Si_2N_2O at the higher temperatures. The transition temperature between them is essentially independent of H_2 concentrations. It is shown by the calculations to be 1477^{o}K with no hydrogen present and drops to 1475^{o} for H_2 contents to 10 percent.

The gaseous species formed in these systems will again be discussed with reference to Figures 9-14. We are now concerned with the right-hand portion of each figure: that showing the calculated

TABLE 5. - INITIAL COMPOSITIONS OF THE SI/N_2/H_2/O_2 SYSTEMS INVESTIGATED

System designation	0 Percent H_2	0.001 Percent H_2	4 Percent H_2	10 Percent H_2	75 Percent H2
N_2, mole	0.999998	0.999988	0.959998	0.899998	0.25
H_2, mole	--------	0.000010	0.04	0.1	0.75
O_2, mole[a]	0.002627	0.002627	0.002627	0.002627	0.002627
Si, mole	0.1	0.1	0.1	0.1	0.1

[a]Total of 2 ppm in the gas and 0.3 w/o in the Si powder.

results for systems composed of $Si/N_2/H_2/O_2$ at temperatures above the beginning of nitridation.

Again, it has been generally conjectured (Lindley et al., 1979; Moulson 1979; Dervisbegovic and Riley 1979) that, despite the details of the mechanisms involved, the primary function of the H_2 is to lower the p_{O_2} and increase the p_{SiO}. In these systems, in contrast to the $SiO_2/N_2/H_2$ systems, the equilibrium partial pressures for both SiO (Figure 9) and O_2 (Figure 10) are unaffected by the additions of up to 10 percent H_2 that are normally added to the nitriding gas. A gas composed of only 25 percent N_2 and 75 percent H_2 does slightly increase the p_{SiO} and reduce the p_{O_2}.

As in the case of p_{SiO}, the p_{Si} is not significantly affected by H_2 content of the nitriding gas (Figure 11). Moreover, under nitriding conditions, the concentration of Si is 4-6 orders of magnitude smaller than the concentration of SiO even with no H_2 present. This, as in the $SiO_2/N_2/H_2$ systems, favors SiO(g) as a source of Si_3N_4 over Si(g).

In contrast to the P_{O_2} and P_{SiO}, the partial pressures of several other species of interest are significantly increased by additions of H_2: H_2O (Figure 12), SiH_4 (Figure 13), and NH_3 (Figure 14). All three are species present in significant amounts. In considering the importance of these results to the actual

nitridation process, it must be kept in mind that these are the amounts of the species present at equilibrium. No conclusion can be made about the amount actually present during the approach to equilibrium.

Other vapor species present in significant amounts (partial pressures $>p_{Si}$) are: H, NH_2, SiH. Of interest also is O which is always present in amounts 4-6 orders of magnitude larger than O_2. With the exception of N, there are no known data or conjectures on the possible roles of these species in the nitridation process. However, any of them could be involved in important intermediate reactions. Work done in the electronics field on production of thin films of silicon nitride on Si wafers using NH_3 has suggested that nascent N from the dissociation of NH_3 should be more active than N_2 (Kamchotka and Ormont 1971). Chen (1980) reported extremely high evaporation losses and formation of large amounts of α-Si_3N_4 whiskers in the reaction vessel after nitridation in NH_3. Reaction kinetics were only semi-quantitative due to the evaporation losses, but the rate of reaction appeared to be slower than in N_2 or N_2 with small amounts of H_2.

Whereas H_2 significantly affects equilibrium composition in the $SiO_2/N_2/H_2$ systems, in amounts of up to 10 percent, it has no effect on compositions in the $Si/N_2/H_2/O_2$ systems (except, of course, for species containing H_2: H_2O, NH_4, SiH_4) at any temperature between 1000^{o} and $2000^{o}K$.

Sintering of Si Powder Compacts

Samples of each of the three powders (high purity Si, high purity Si + 1 percent Fe and lower purity Si) were sintered for 5h at 1375°C in either He or H_2. Weight loss due to evaporation during sintering and surface area before and after sintering are listed in Table 6. As-compacted surface areas were ~7m^2/g for all three powders. In all cases the surface area decreased during sintering, with particle growth being greater in He than in H_2.

Fracture surfaces of each sintered specimen were examined by SEM and polished cross-sections by light microscopy. The as-compacted microstructures are shown in Figure 15. Consider first the high purity Si. Figures 16 and 17 show that H_2 has the effect of preventing the growth of extremely large particles in high purity Si powder except at the surface of the compact. Surface area of the green powder compact was 7.01m^2/g. This was reduced to 3.00m^2/g in H_2 and 0.42m^2/g in He. Except for the near-surface region of the H_2-sintered compact, the structures of both types of specimens appear to be quite uniform. The He-sintered compact does not have an enlarged edge region.

The microstructures produced by the addition of Fe mixed heterogeneously into the high purity Si powder are shown in Figures 18 and 19. The structure after sintering in He is still very large (surface area = 0.2m^2/g) and uniform (Figures 18a and 19a), unlike the nonuniform structure observed by Arundale and Moulson (1977)

TABLE 6. - WEIGHT LOSS AND SURFACE AREA OF Si POWDER COMPACTS SINTERED 5h AT 1375° C

Atmosphere	High purity Si		High purity Si + Fe		Low purity Si	
	Weight loss, percent	Surface area, m^2/g	Weight loss, percent	Surface area, m^2/g	Weight loss, percent	Surface area, m^2/g
(As compacted)	---	7.01	---	6.99	---	6.77
H_2	5.3	3.00	5.8	0.96	2.8	0.91
He	1.4	0.42	1.5	0.22	2.0	0.84

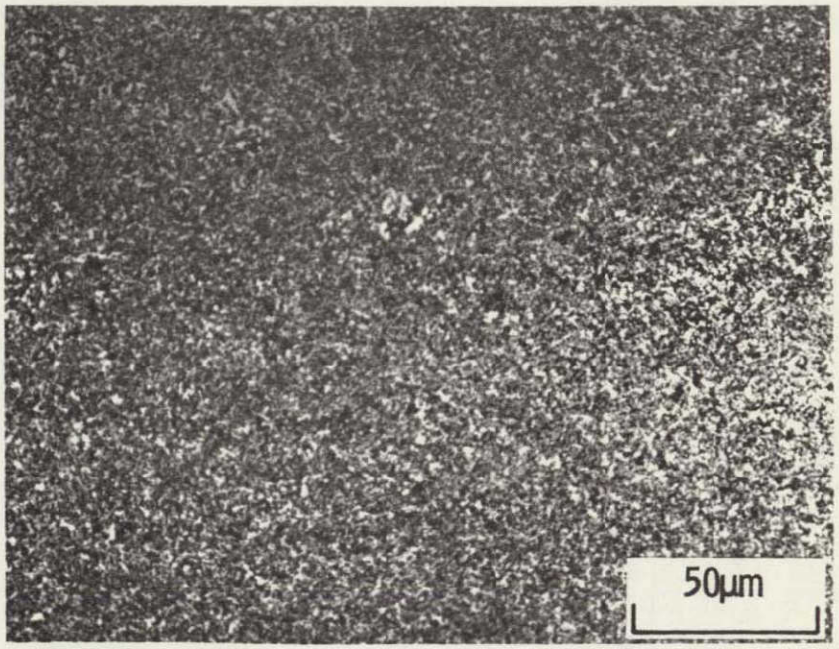

a. High purity Si

Figure 15. Light micrographs of polished section of as-compacted Si

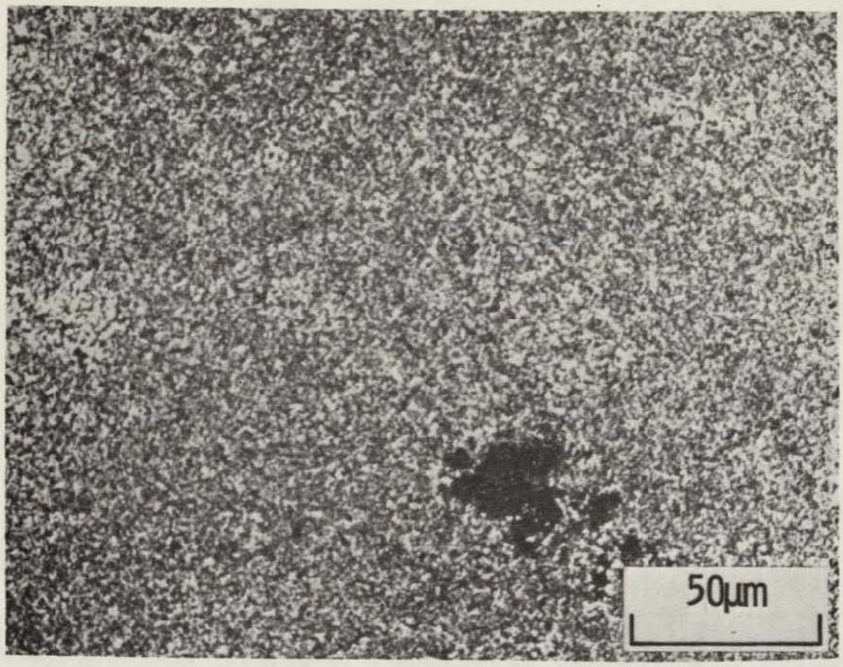

b. High purity Si + 1 percent Fe

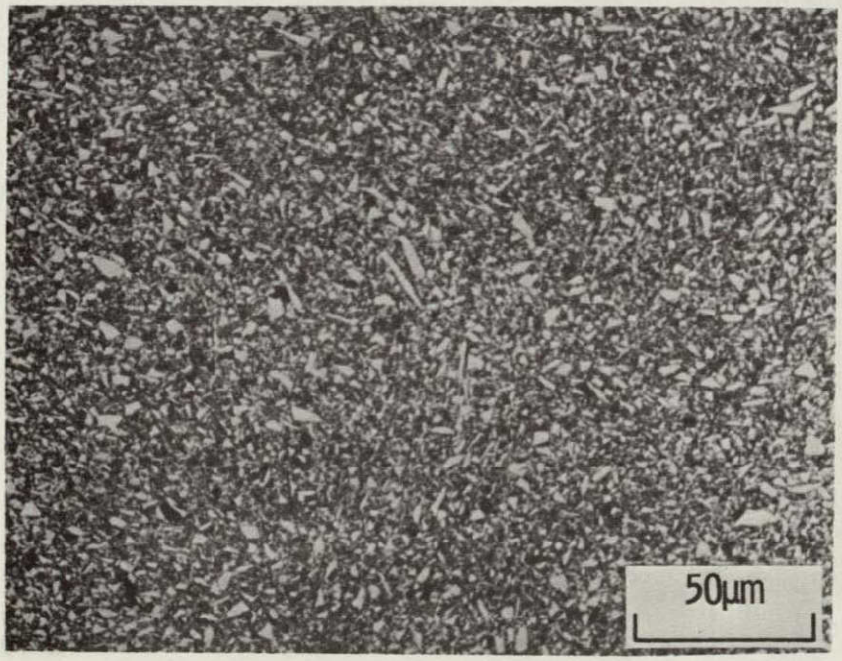

c. Lower purity milled Si

Figure 15. (Continued)

ORIGINAL PAGE IS
OF POOR QUALITY

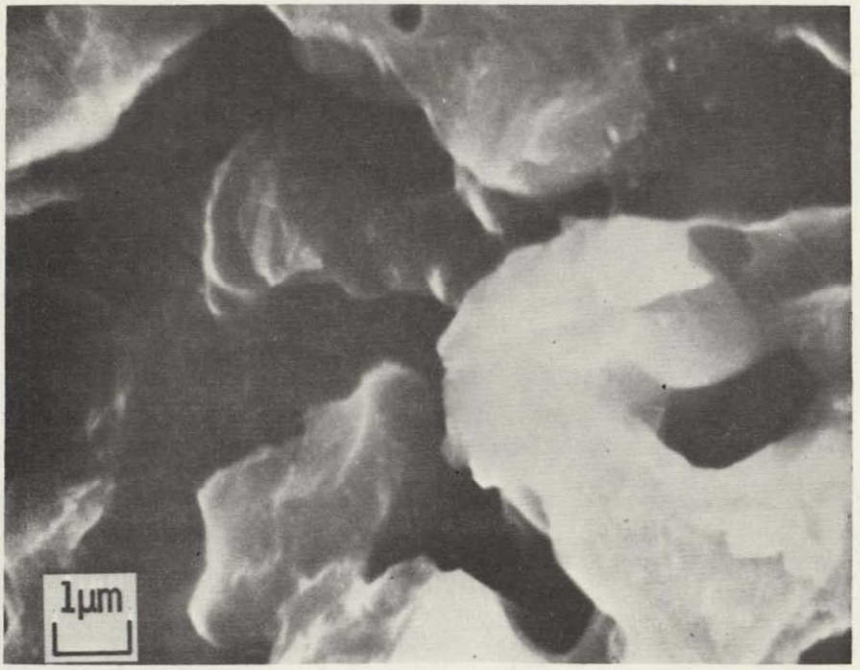

a. Sintered in He

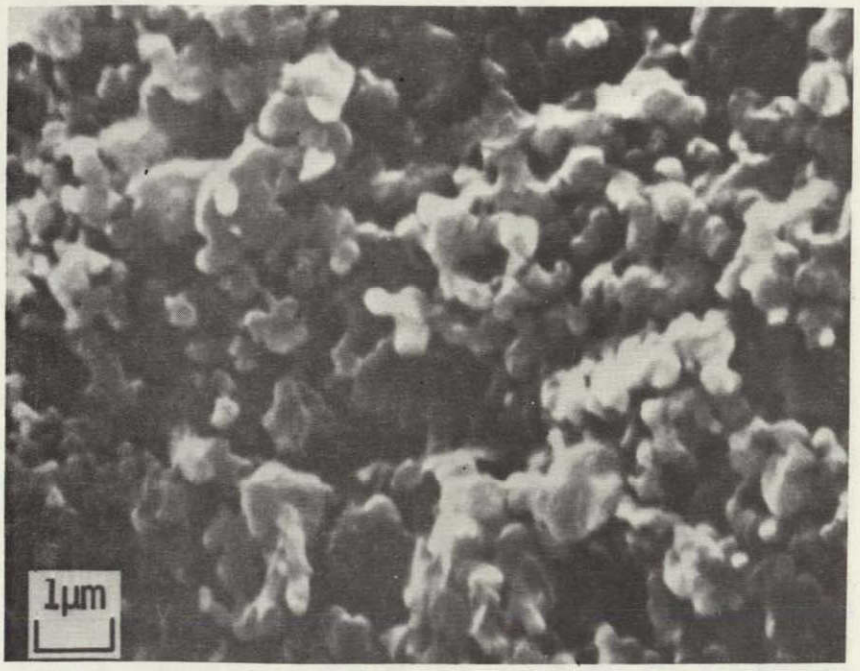

b. Sintered in H_2

Figure 16. SEM micrograph of high purity Si powder sintered 5h, 1375°C

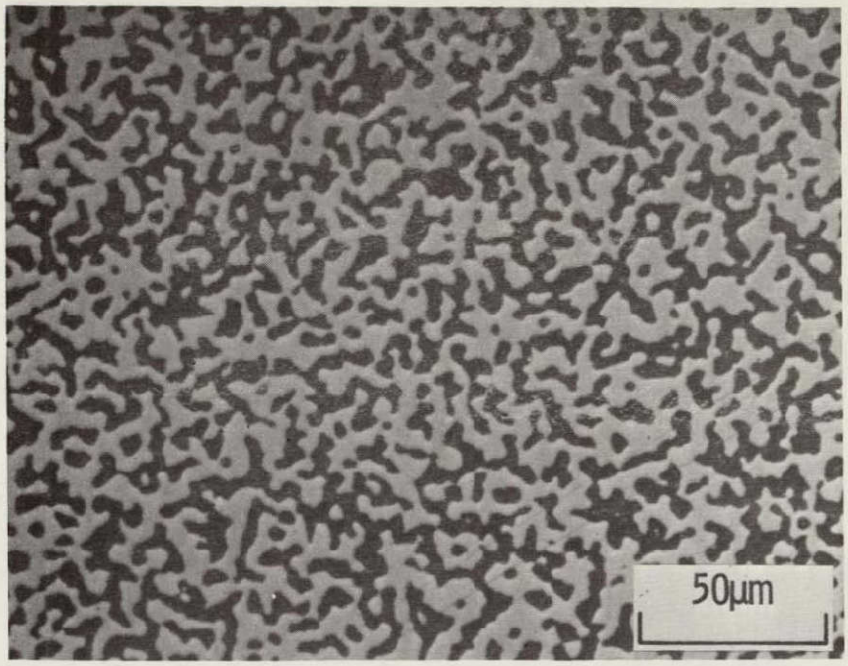

a. Sintered in He

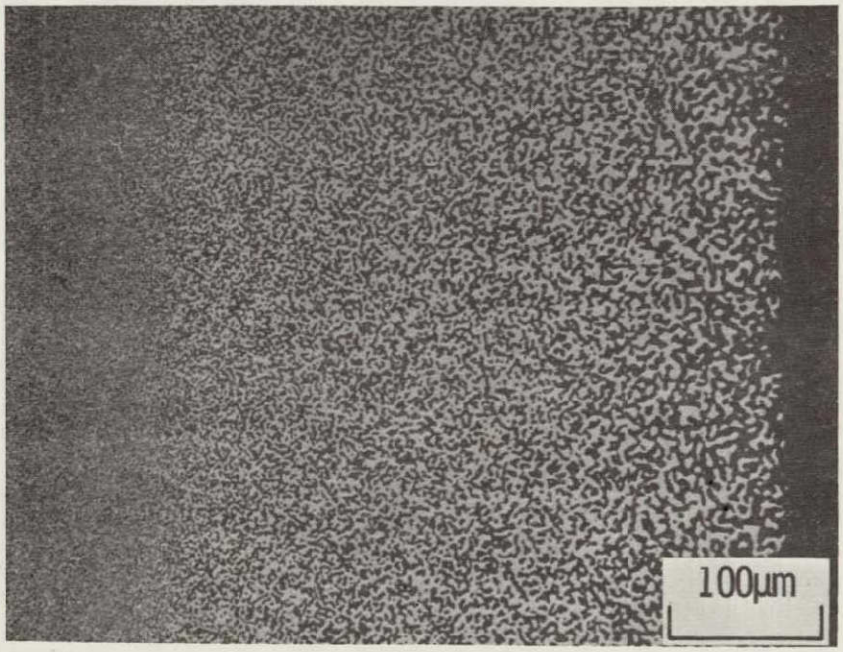

b. Sintered in H_2

Figure 17. Light micrograph of polished section of high purity Si sintered 5h, 1375°C

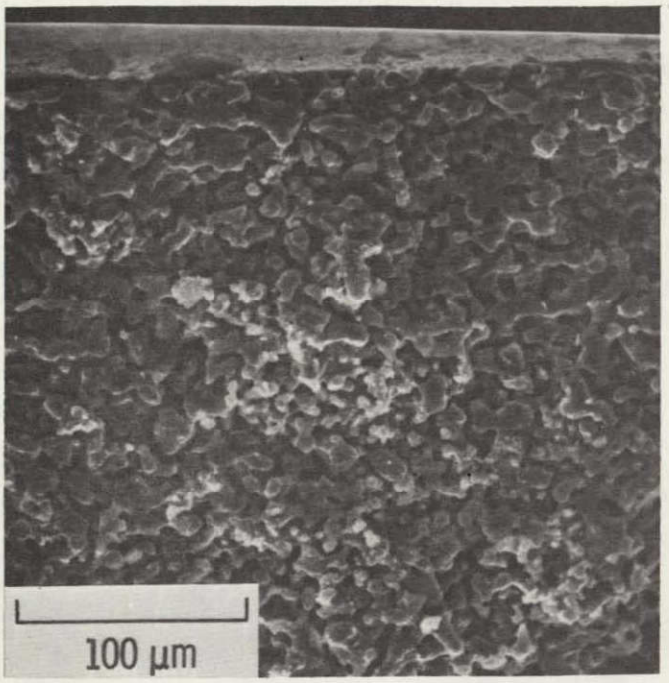

a. Sintered in He

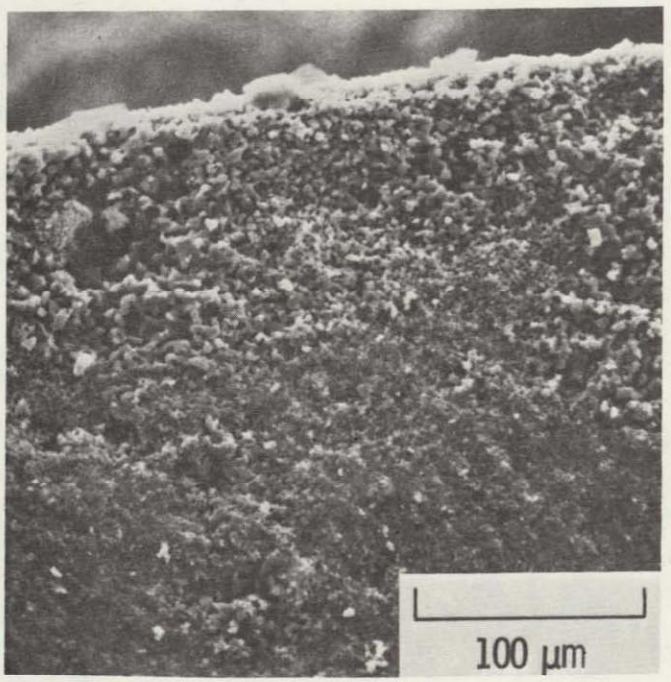

b. Sintered in H_2

Figure 18. SEM micrographs of high purity Si + 1 percent Fe sintered 5h, 1375^{o}C

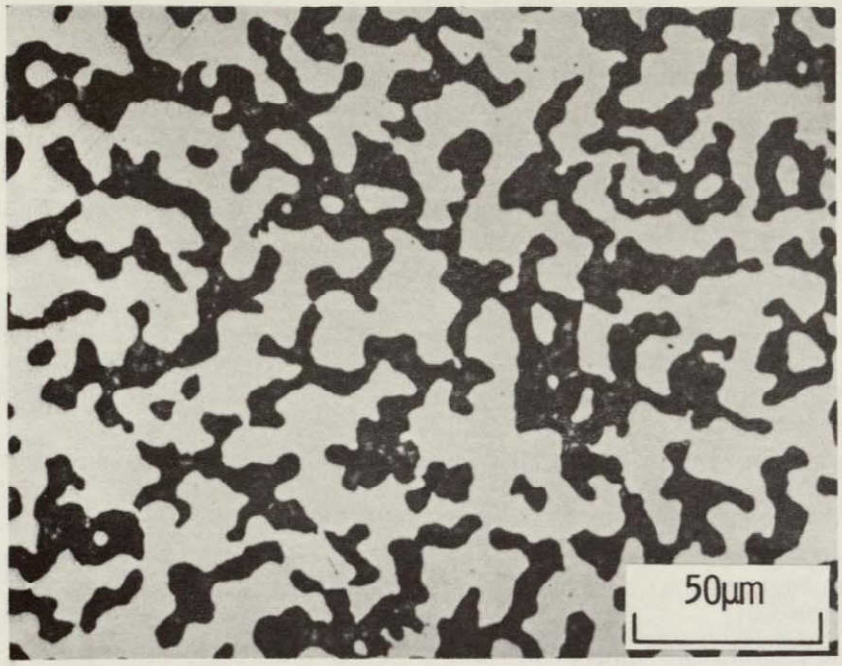

a. Sintered in He

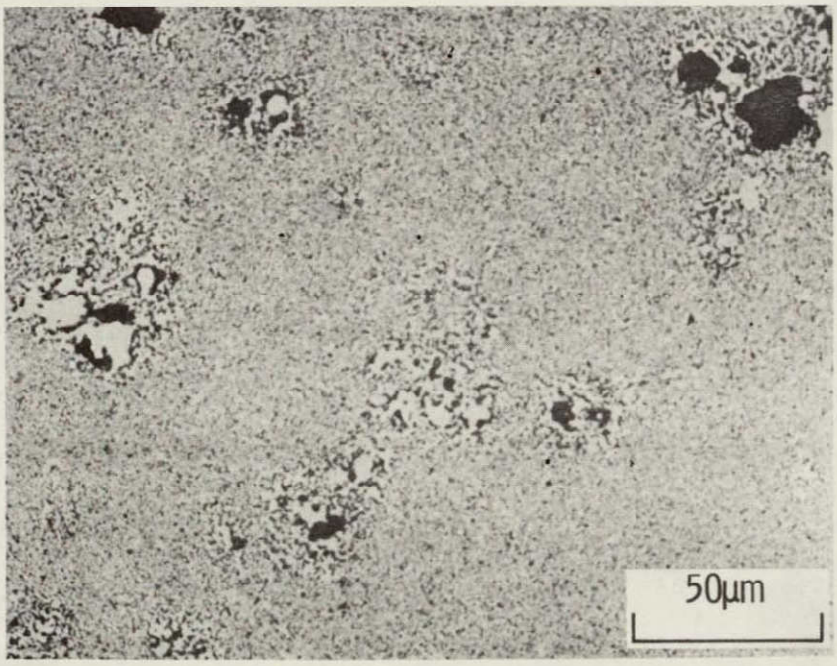

b. Sintered in H_2

Figure 19. Light micrographs of high purity Si + 1 percent sintered 5h, 1375°C

after argon sintering and attributed to local melting of $FeSi_2$. The microstructure of the compact sintered in H_2 is predominantly still quite fine, but contains regions of very large particles (Figure 18b and 19b). Overall surface area is $0.96 m^2/g$, much less than that of the high purity Si without Fe sintered in H_2. Energy dispersive x-ray analysis of these regions indicates the presence of Fe at these large particles, whereas Fe is absent in the finer regions. The large particles growth adjacent to the surface can be seen in Figure 18b.

The lower purity milled powder contains a more uniform distribution of Fe and other impurities and the H_2- and He-sintered microstructures are quite similar (Figures 20 and 21). Particle growth of the compact sintered in He (Figure 20a and 21a) was slightly less than for the high purity powder and the structure is still fairly uniform. (Variations in grain size probably reflect the varying initial particle sizes.) The average particle size of the compact sintered in H_2 ($0.913 m^2/g$) (Figure 20b and 21b) is approximately the same as that in He but contains high-Fe regions of even larger particles. Both samples of this material have a region of large grain growth near the surface. The rather sharp interface between the coarse and fine regions can be seen in Figure 21.

The structures developed in high purity Si during sintering in He and H_2 are similar and characteristic of matter transport by either evaporation/condensation or surface diffusion. Both of these

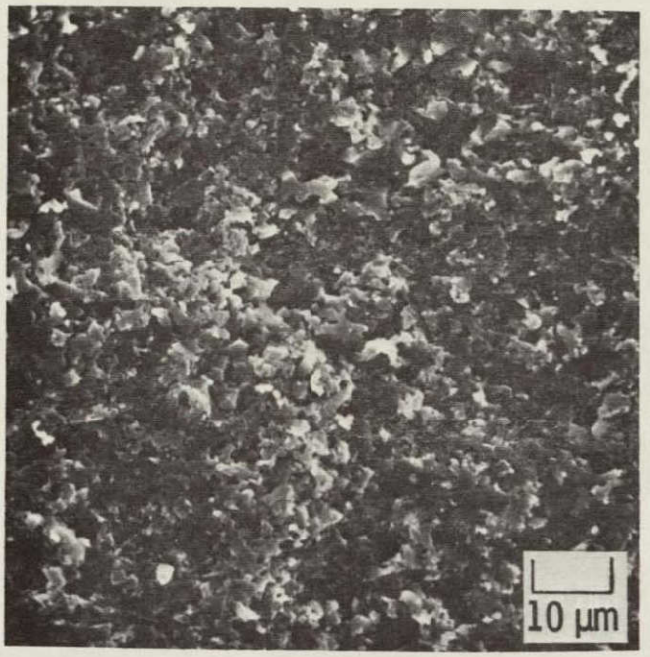

a. Sintered in He

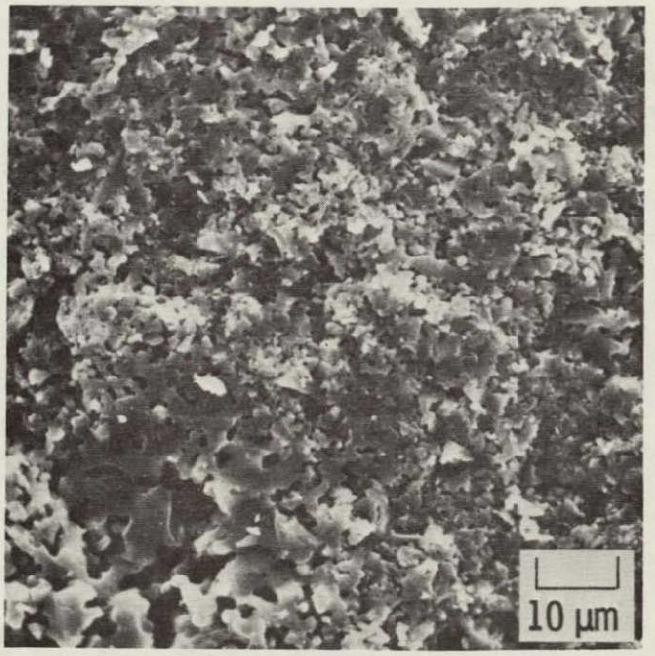

b. Sintered in H_2

Figure 20. SEM micrographs of lower purity milled Si powder sintered 5h, 1375^{o}C

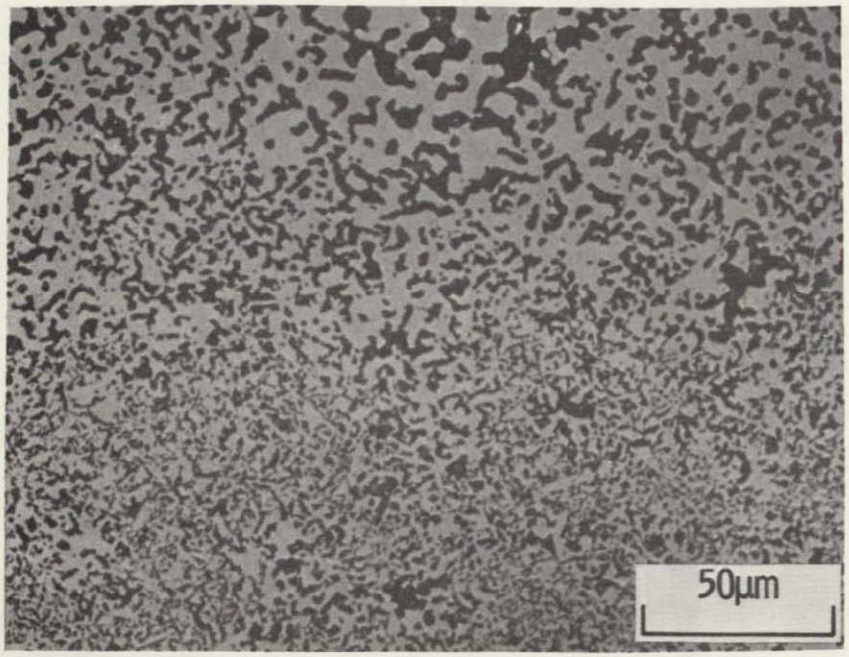

a. Sintered in He

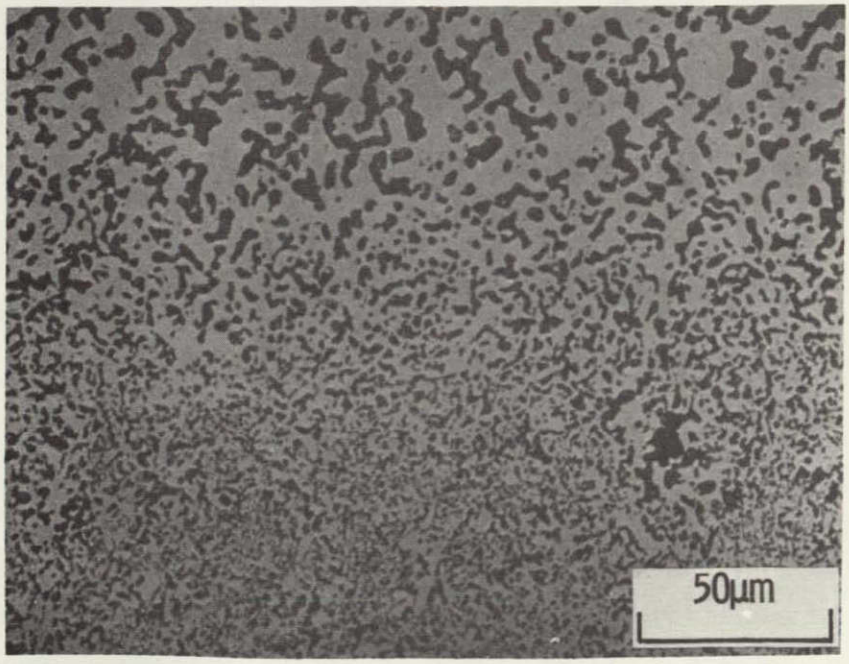

b. Sintered in H_2

Figure 21. Light micrographs of polished sections of lower purity milled Si compact sintered 5h, 1375^{o}C

processes result in particle consolidation and neck formation, but little or no densification. While both structures are similar in appearance, there is much less grain growth in H_2 than in He, indicating that H_2, in some manner, suppresses matter transport.

Whether the inhibition of grain growth of the high purity Si powder during sintering in H_2 is actually a general effect of the H_2 or due to the nature of the powder is unknown. Welsch, Moller and Heuer (1980) have reported some densification, but little grain growth during sintering and annealing at 1380^{o}C of a Si powder similar in size and purity, but initially amorphous, in both vacuum and hydrogen/argon. They speculated that the silica film surrounding each Si particle could inhibit grain growth (1981). Makaviecki and Holt (1979) reported that surface diffusion studies of single crystal Si wafers indicated that oxide films on silicon essentially stops surface diffusion. They found these oxide films extremely stable and particularly difficult to remove from surfaces in close contact suggesting that this might offer an explanation for the difficulty in densifying Si powder compact. Greskovich and Rosolowski (1976) sintered both the fines from a crushed and acid leached Si powder and an extremely fine silane derived powder in argon and concluded that vapor transport, not surface diffusion was the dominant mechanism of neck formation in non-densifying Si.

The SiO_2 layer on the Si particles may provide a path of rapid matter transport, especially at this high sintering temperature,

either through the SiO_2 itself or at the Si/SiO_2 interface. H_2-enhanced removal of this path could then inhibit sintering. Physi-or chemisorption of H_2 on the Si surface after SiO_2 removal could also suppress surface diffusion or evaporation/condensation and inhibit grain growth and neck formation.

When Fe is added to the high purity powder, the high-Fe regions show not only extensive particle growth and neck formation but also areas of high density. Some Fe and other metallic impurities are present in the Si itself. Glasgow (1980) has shown that, during sintering of Si, the metallic impurities migrate to the surface of the Si particles. Other impurities come from the wear of mill components during processing of the Si powder. It is assumed that these particles are largely in the form of a metallic oxide, iron being present, for example, as Fe_2O_3. Reduction of the Fe_2O_3 to FeO by H_2 presents the possibility of the formation of low melting point silicates especially in the presence of trace amounts of other metallic oxides likely to be present. Formation of these silicate phases then provides a route for densification of the high-Fe regions of the compact by liquid phase sintering.

Nitridation of Si Powder Compacts

The conditions under which samples of the three Si powders were nitrided are shown in Table 7. Also listed are the weight gain and

TABLE 7. - WEIGHT GAIN AND α/β RATIO OF Si_3N_4

Atmosphere		Nitridation temperature, °C					
Heat	Nitride	1200	1375	1200	1375	1200	1375
		High purity Si		High purity Si + 1 percent Fe		Low purity Si	
N_2	N_2						
Percent weight gain		~3	20.3	~9	65.2	15.9	62.2
α/β-Surface		----	2.9	----	3.8	3.6	2.7
α/β-Powder from cross section		1.9	1.9	2.3	2.2	----	----
N_2/1 percent H_2	N_2/1 percent H_2						
Percent weight gain		----	----	----	----	23.6	62.3
α/β-Surface		----	----	----	----	3.2	3.0
α/β-Powder from cross section		----	----	----	----	----	----
N_2/4 percent H_2	N_2/4 percent H_2						
Percent weight gain		25.7	43.2	34.0	62.7	33.9	~60
α/β-Surface		----	5.2	----	5.0	4.3	4.7
α/β-Powder from cross section		2.1	1.8	3.2	2.6	----	----
He	N_2						
Percent weight gain		----	2.8	----	7.7	11.9	14.0
α/β-Surface		----	----	----	----	2.2	0.4
α/β-Powder from cross section		----	0.7	----	1.6	----	----
He	N_2/1 percent H_2						
Percent weight gain		----	----	----	----	18.9	21.1
α/β-Surface		----	----	----	----	2.7	0.4
α/β-Powder from cross section		----	----	----	----	----	----
He	N_2/4 percent H_2						
Percent weight gain		----	9.5	----	16.8	30.2	32.9
α/β-Surface		----	----	----	----	3.9	0.8
α/β-Powder from cross section		----	1.1	----	2.0	----	----
H_2	N_2						
Percent weight gain		----	8.6	----	32.5	----	14.1
α/β-Surface		----	2.0	----	4.4	----	2.0
α/β-Powder from cross section		----	----	----	----	----	----

the ratio of α-Si_3N_4 to β-Si_3N_4 (α/β ratio). Weight gains (degree of nitridation) are less at 1200°C than at 1375°C while α/β ratios are usually higher. In general, at either temperature, weight gains and α/β ratios increase as Si purity decreases. The α/β ratios of the lower purity Si heated in He to 1375°C, to be discussed later, are an exception, all being very low. That α/β ratio is also higher at the compact surface than in the interior.

Nitrided weight gains and α/β ratios for the lower purity powder after the compacts were nitrided under four different conditions are shown in Figures 22-25. It can clearly be seen from these figures that both the α/β ratio and degree of nitridation (percent weight gain) of this powder increase with increasing H_2 added to the nitriding gas. The compacts nitrided at 1375°C for 4 hours with the heating and cooling portions of the cycle in N_2/H_2 (Figure 24) were all fully nitrided. Theoretical weight gain of fully nitrided Si is 66.7 percent, but due to vaporization losses, actual weight gains of completely nitrided compacts (<1 percent residual Si by X-ray diffaction) are on the order of 60-62 percent. Weight gains under the other conditions indicated only 30-50 percent nitridation.

Samples heated in He had less Si_3N_4 than those heated in N_2 or N_2/H_2, partially a result of less actual nitridation time. The usual assumption that α is the low temperature form and β

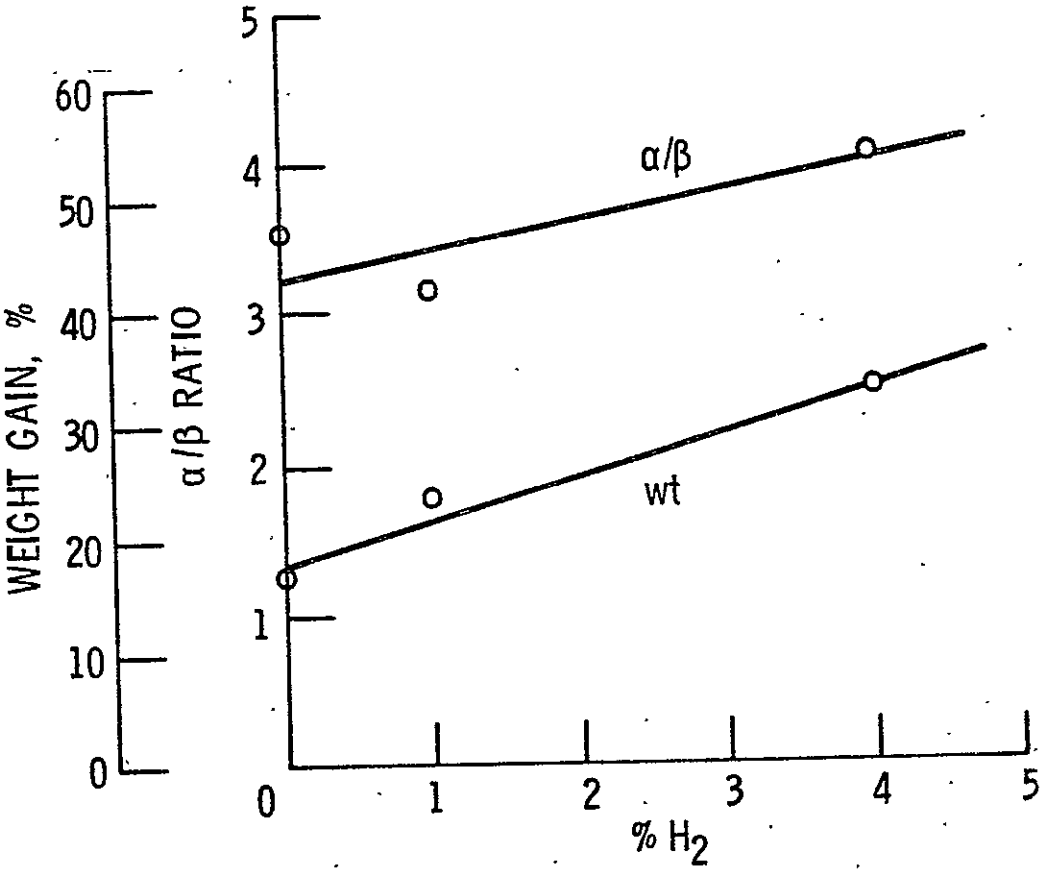

Figure 22. - α/β ratio and weight gain of nitrided lower purity Si powder as a function of H_2 content of the nitriding gas. 4h, 1200° C, heated and cooled in the nitriding atmosphere.

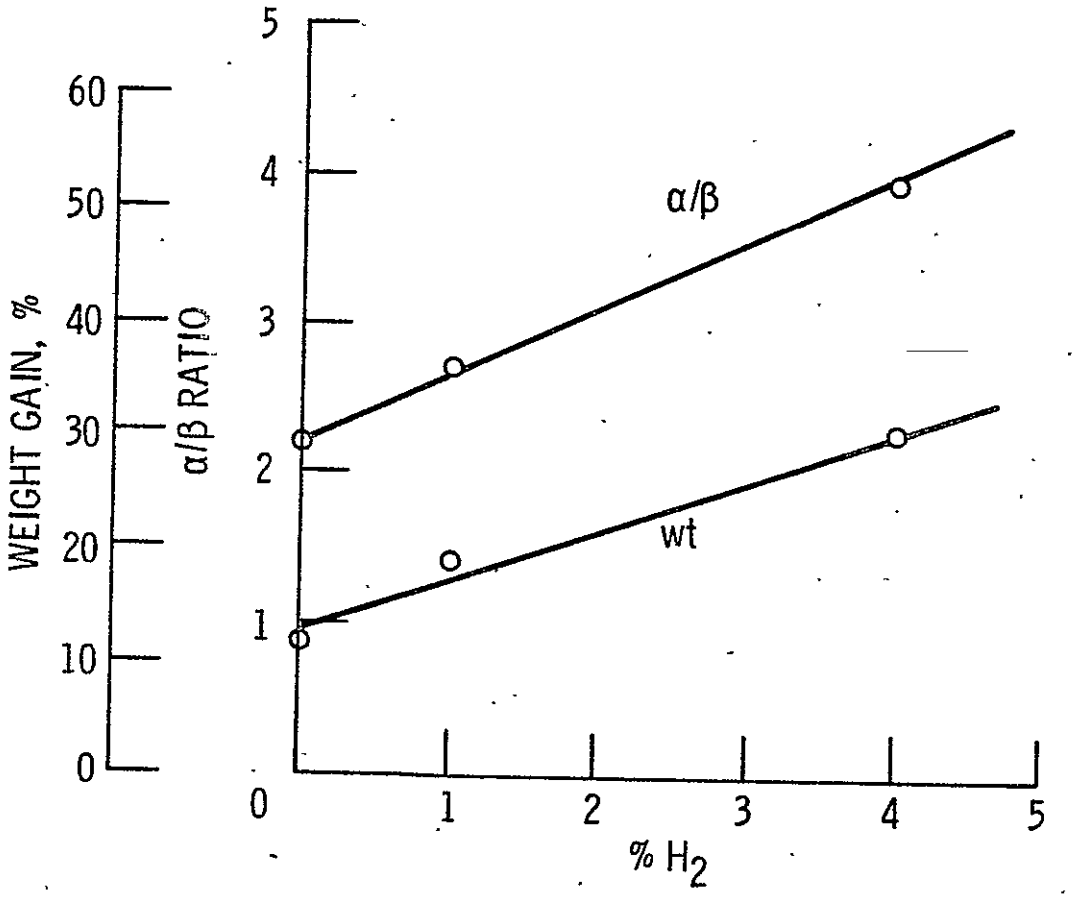

Figure 23. - α/β ratio and weight gain of nitrided lower purity Si powder as a function of H_2 content of the nitriding gas. 4h, 1200° C, heated and cooled in He.

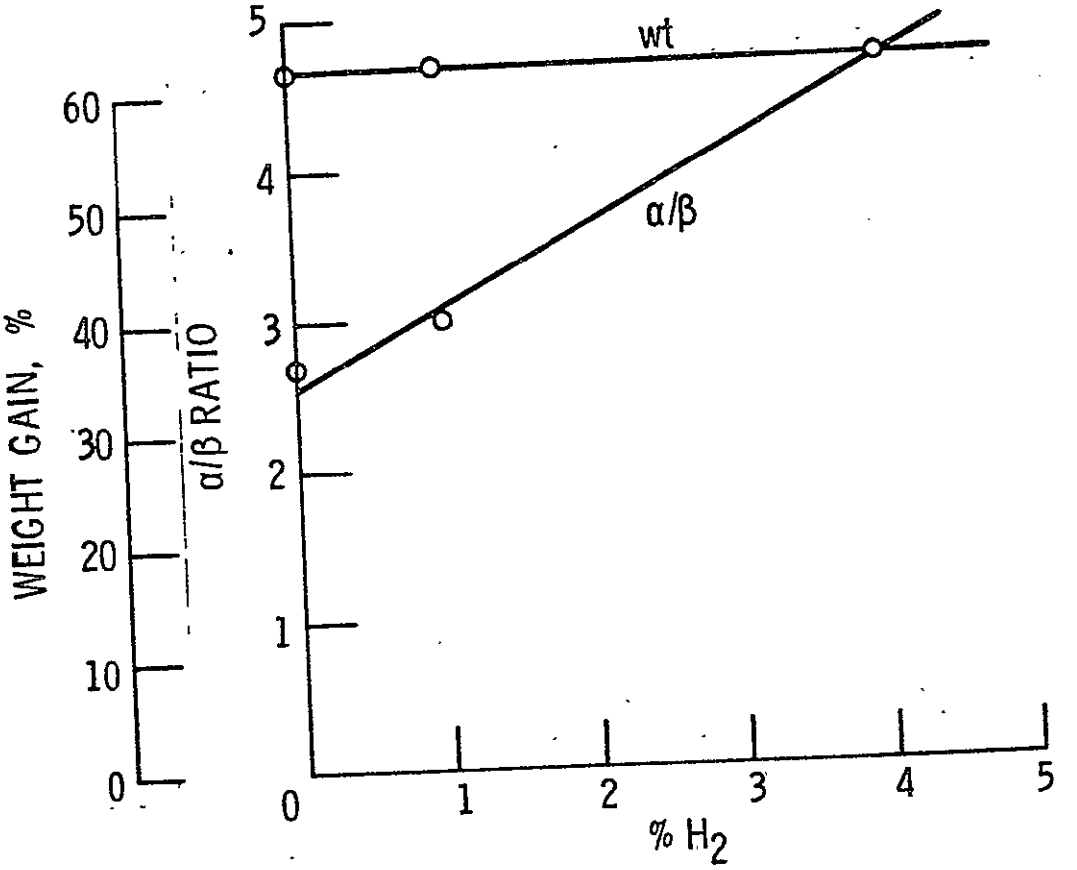

Figure 24. - α/β ratio and weight gain of nitrided lower purity Si powder as a function of H_2 content of the nitriding gas. 4h, 1375° C, heated and cooled in the nitriding atmosphere.

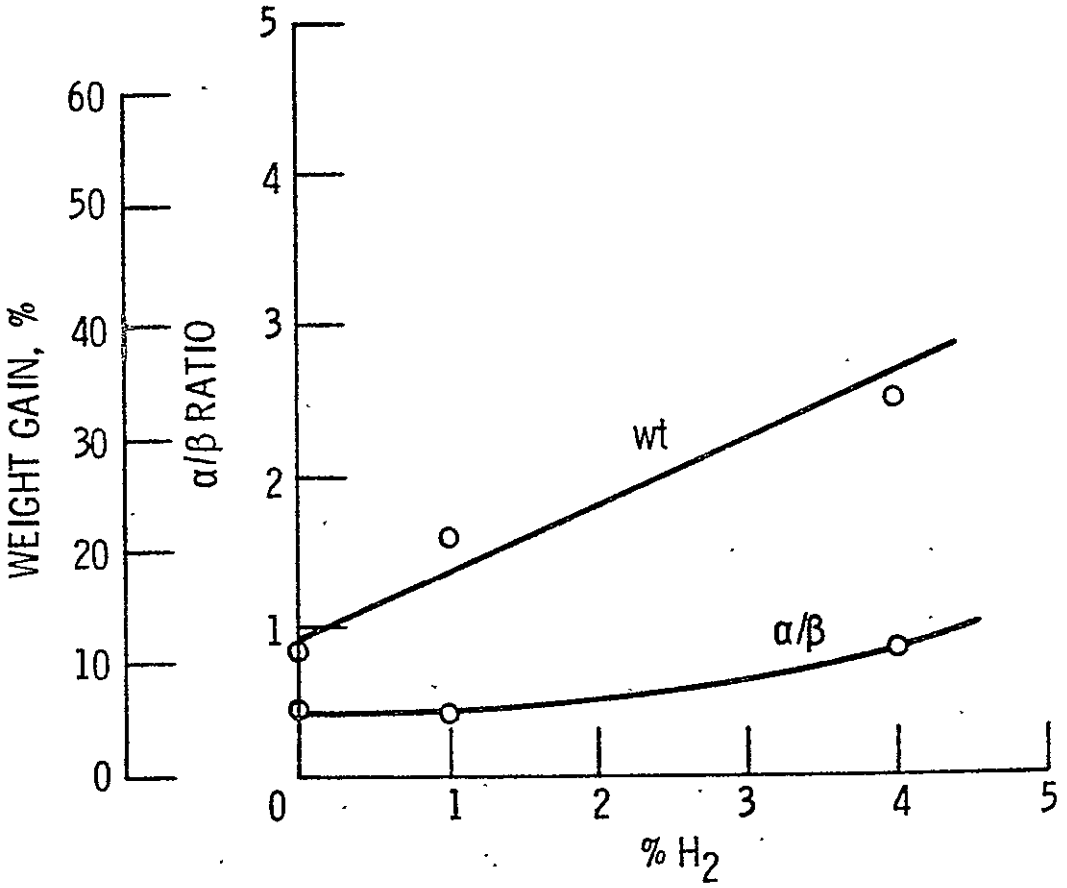

Figure 25. - α/β ratio and weight gain of nitrided lower purity Si powder as a function of H_2 content of the nitriding gas. 4h, 1375° C, heated and cooled in He.

the high temperature form (apparently supported by both thermodynamic data (Hendry 1976) and experiment (Morgan 1980)) would lead to a lower α/β ratio for those samples heated to the nitridation temperature in He compared with samples where nitridation began at lower temperatures. This difference is not too great at 1200°C (Figures 22 and 23) since little nitridation occurs below that temperature, but at 1375°, the differences are significant. As noted above, the samples in N_2 or N_2/H_2 for the full cycle are all fully nitrided with α/β ratios increasing from 2.7 to 4.7 with increasing H_2 content. The specimens heated to 1375° in He and then nitrided (Figure 25) had weight gains of only 11 to 30 percent depending on H_2 content. The α/β ratios of these samples were all less than 1, apparently confirming that much of the α-Si_3N_4 usually present forms at temperatures lower than 1375°C.

As can be seen in Figure 26, the nitrided structures after nitridation at 1375°C following heating in N_2/4 percent H_2 (Figure 26a) or in He (Figure 26b) are very different. The sample heated in N_2/H_2 began nitriding at low temperatures while the Si particles were still small and formed large amounts of fine-grained α-mat. The sample heated in He, however, sintered to a very large grain size which could not be fully nitrided. It is still not clear whether the difference in α/β ratio is really because α-Si_3N_4 is

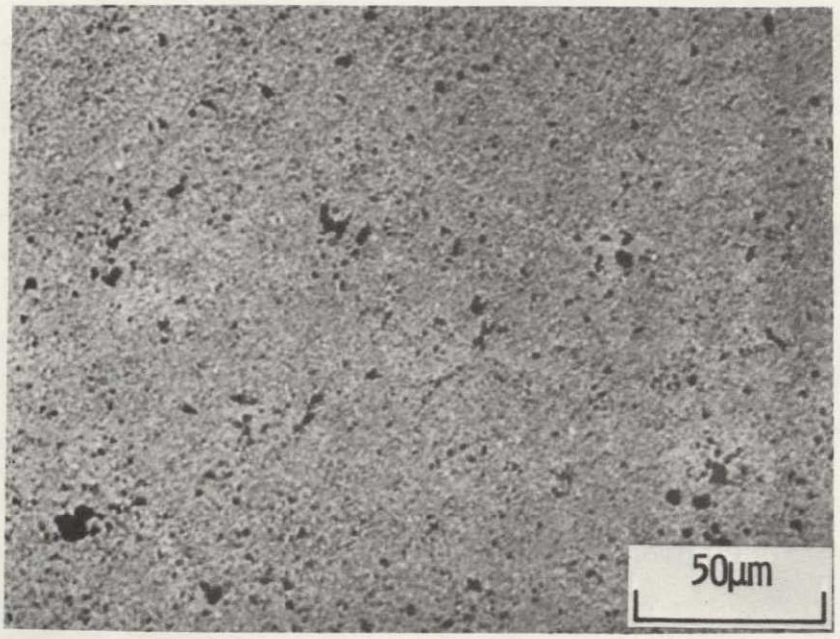

a. Heated in N_2/4 percent H_2

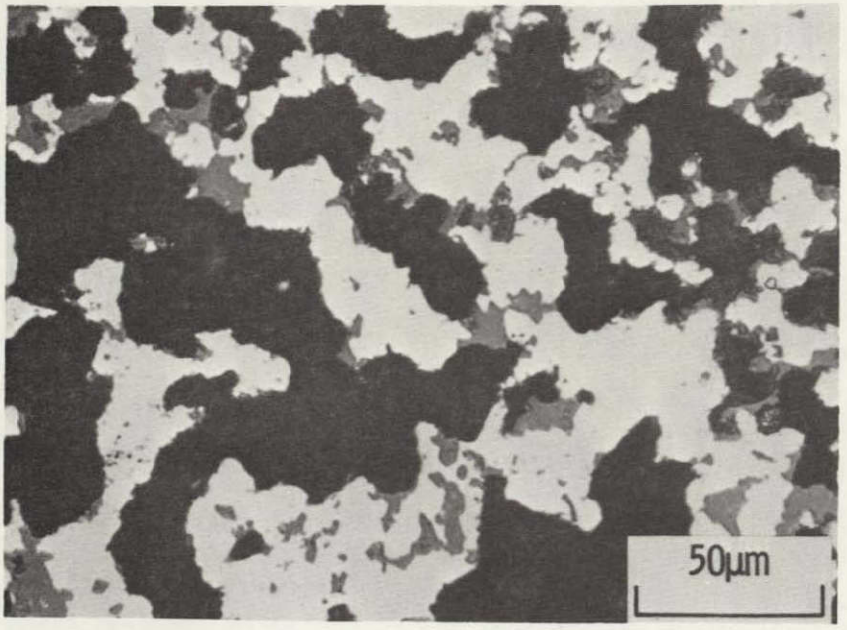

b. in Heated in He

Figure 26. Micrograph of polished section of Si_3N_4 from lower purity Si compact nitrided in N_2/4 percent H_2, 4h, 1375°C white-Si, black-porosity, grey-Si_3N_4

a low temperature form and β-Si_3N_4 is a high temperature form. Since α-Si_3N_4 is assumed to form largely by vapor phase reactions and β-Si_3N_4 directly on the Si surface, the amount of surface area at nitridation may be a contributing factor.

SEM micrographs (Figure 27) of the fully nitrided compacts of this powder suggest that the particle size and porosity do become finer and more uniformly distributed as the H_2 content is increased. This effect is presumably the result of H_2 suppressing grain growth and increasing the concentration of Si-containing vapor species. Figures 27a (N_2) and 27b (N_2/1 percent H_2) both show large grains and very porous regions. The porosity in Figure 27c (N_2/4 percent H_2) appears to be more uniform in size and more uniformly distributed.

The SEM micrographs in Figure 28 show that this refinement in the microstructure occurs early in the nitridation process. These bars were nitrided at 1200°C and had weight gains of only 16-34 percent. Figure 28a (nitrided in N_2) is composed of large Si grains with some fine-grained material beginning to fill the pores. With 4 percent H_2 added (Figure 28c), the structure is predominantly very fine grained with few remaining large Si grains and no large porosity.

The behavior of this powder, e.g., the trends in completeness of nitridation and α/β ratio with H_2 content, the microstructural development, etc., was as expected from published nitridation

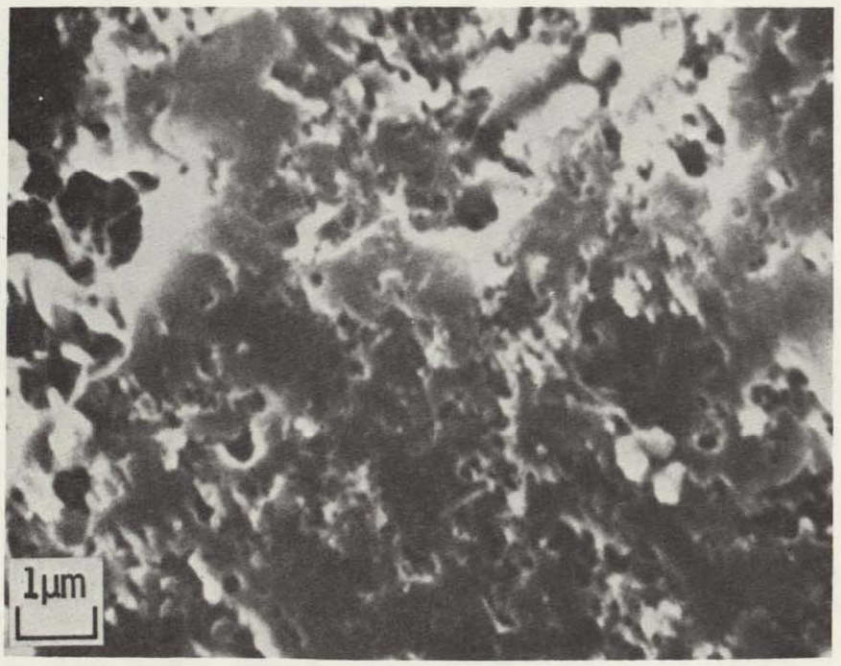

a. in N_2

Figure 27. SEM micrographs of fracture surface of Si_3N_4 from lower purity Si compact nitrided 4h, 1375°

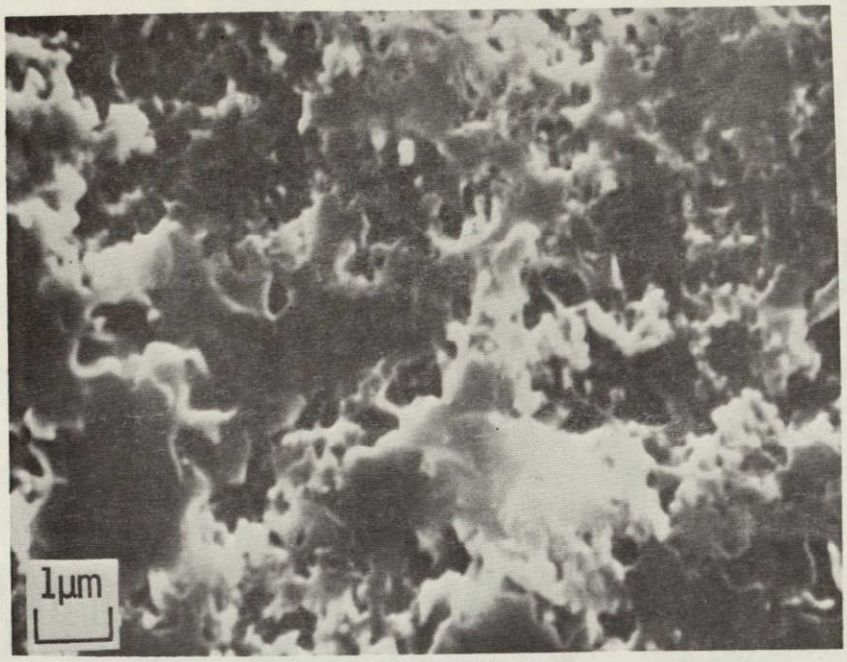

b. in N_2/1 percent H_2

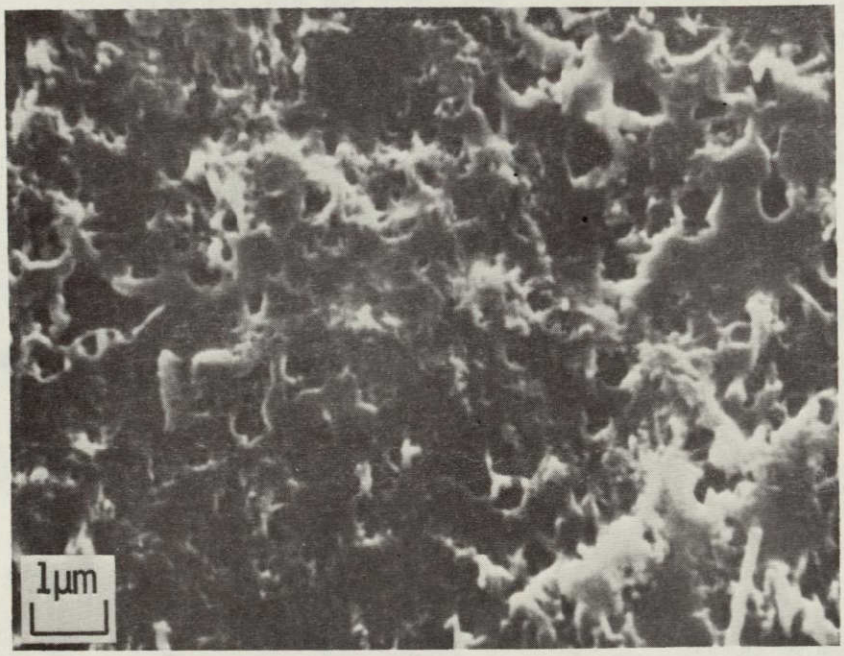

c. in N_2/4 percent H_2

Figure 27 (Continued)

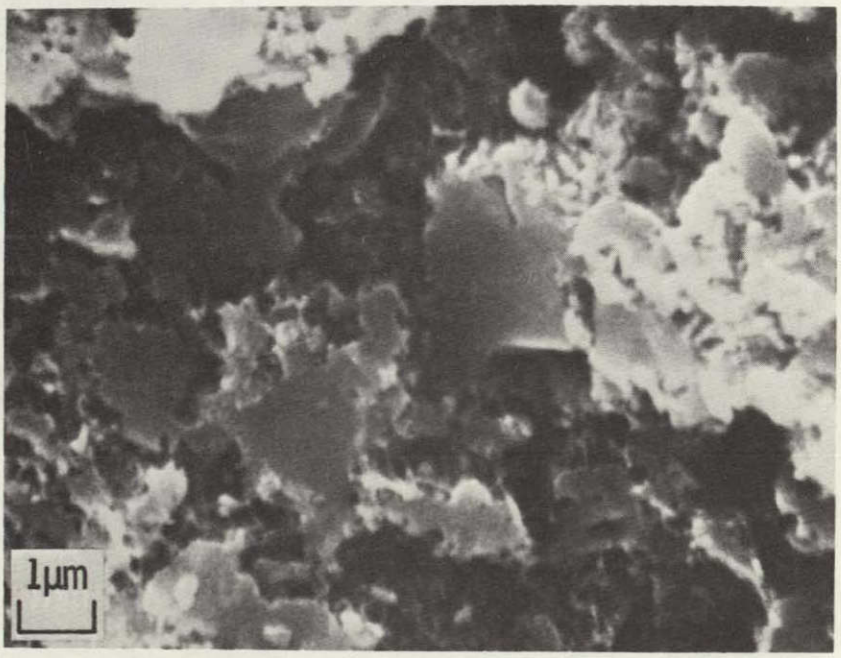

a. in N_2.

Figure 28. SEM micrographs of fracture surface of Si_3N_4 made from lower purity Si powder compact nitrided 4h at 1200°C

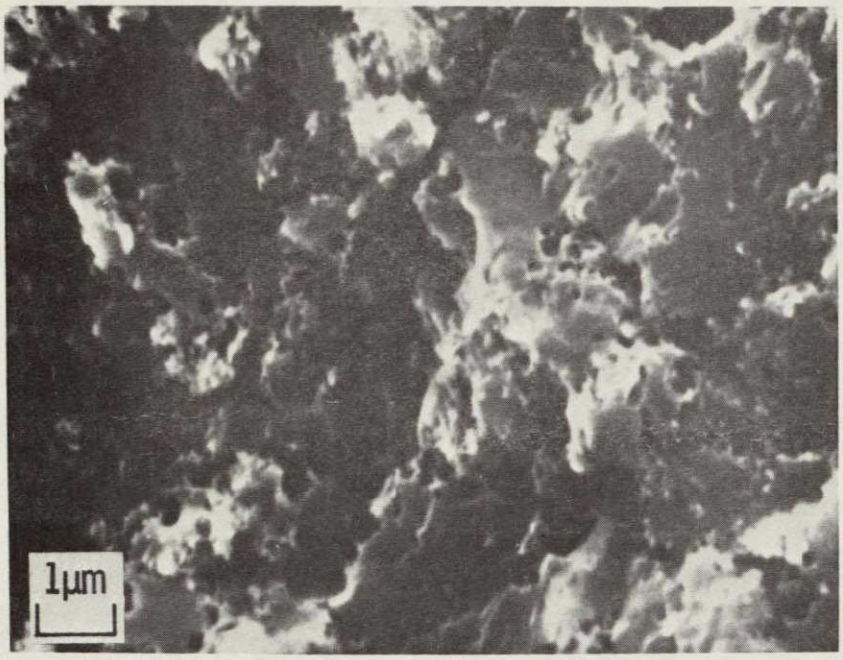

b. in N_2/1 percent H_2

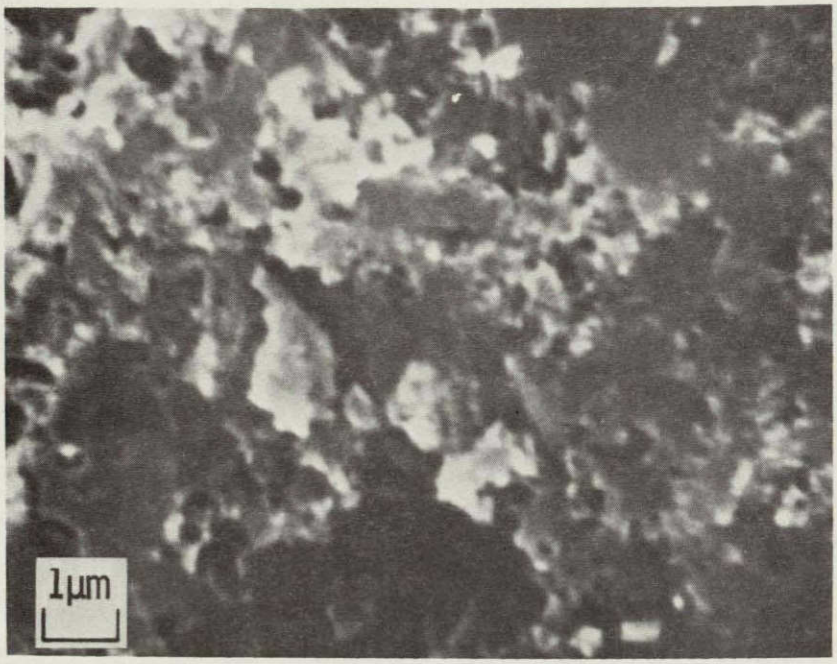

c. in N_2/4 percent H_2

Figure 28 (Continued)

studies. Most of the studies reported in the literature, while done under a variety of conditions, involved Si powders of purity similar to this low purity powder. Nitriding atmospheres and furnace components were also similar. However, a high purity Si powder doesn't behave quite so predictably. A more complete picture of what is really happening during nitridation might be gained by looking at the separate and combined effects of H_2 and Fe.

Samples of both the pure and Fe-containing high purity Si green compacts were nitrided together at 1200° or 1375°C in either N_2 or N_2-4 percent H_2. Results in Table 7 are shown in Tables 8 and 9. In all cases, the Fe-containing Si had a higher weight gain much larger amount of α, nearly the same amount of β, much less free Si and a higher α/β ratio. The microstructure were also considerably different.

At 1200°, H_2 had a much greater effect than Fe on the degree of reaction, but Fe had a greater effect in increasing the α/β ratio. There was almost no nitridation in N_2 of either the pure or Fe-containing Si. However, in N_2/4 percent H_2 the pure and Fe-containing Si had weight gains of 26 percent and 34 percent respectively. The expected increase in α/β ratio with H_2 (Lindley et al. 1979) did not occur in the pure Si, both samples having $\alpha/\beta \approx 2$. An increase was seen, however, in the Fe-containing samples with α/β ratio increasing from 2.3 to 3.2.

TABLE 8

Results of nitridation of high purity Si at 1200°C in N_2 or N_2/4 percent H_2

		N_2	$N_2/4H_2$
Si	wt gain, percent	~3	25.7
	percent α	24	41
	percent β	13	19
	percent retained Si	63	40
	α/β	1.9	2.1
Si+ 1 percent Fe	wt gain, percent	~9	34
	percent α	31	58
	percent β	13	18
	percent retained Si	56	24
	α/β	2.3	3.2

TABLE 9

Results of nitridation of high purity Si at 1375°C in N_2 or N_2/4 percent H_2

		N_2	$N_2/4H_2$
Si	wt gain, percent	20.3	43.2
	percent α	53	59
	percent β	28	32
	percent retained Si	20	8
	α/β	1.9	1.8
Si+ 1 percent Fe	wt gain, percent	65.2	62.7
	percent α	68	71
	percent β	31	28
	percent retained Si	1	1
	α/β	2.2	2.6

At 1375°, addition of H_2 to the N_2 increased the degree of nitridation of the pure Si with the weight gain increasing from 20 percent to 43 percent. Again, there was no effect on the α/β ratio. Both Fe-containing samples were nearly fully nitrided with the one in H_2 again having a slightly higher α/β ratio.

The most significant effects of Fe are on the morphology of the RBSN. The pure Si samples show no signs of Si_3N_4 whiskers within the compact[1] at both temperatures and in both atmospheres. All Fe-containing samples have whiskers. Figures 29-32 show examples of each structure. In each figure, the Si + Fe sample is typical of an RBSN fracture surface with transgranular fracture of regions containing fine porosity and whiskers growing into the larger pores. The pure Si sample in each figure shows only interparticle fracture. The Si particles appear to have nitrided individually with little evidence of interparticle bonding.

High purity Si powder nitrided in either N_2 or N_2/4 percent H_2 shows no sign of the whiskers or fine grained-mat usual to RBSN. Both α- and β-Si_3N_4 are apparently formed on and within the Si particles creating little interparticle bonding and

---

[1]Whisker growth usually observed on the surfaces of powder compacts and single crystal wafers is thought to be nucleated by metallic contaminants from the furnace tube and hardware.

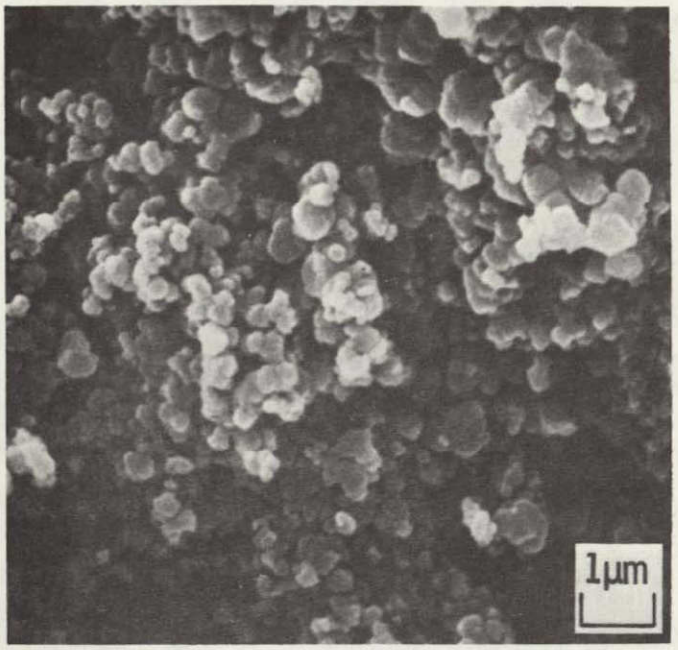

a. High purity Si

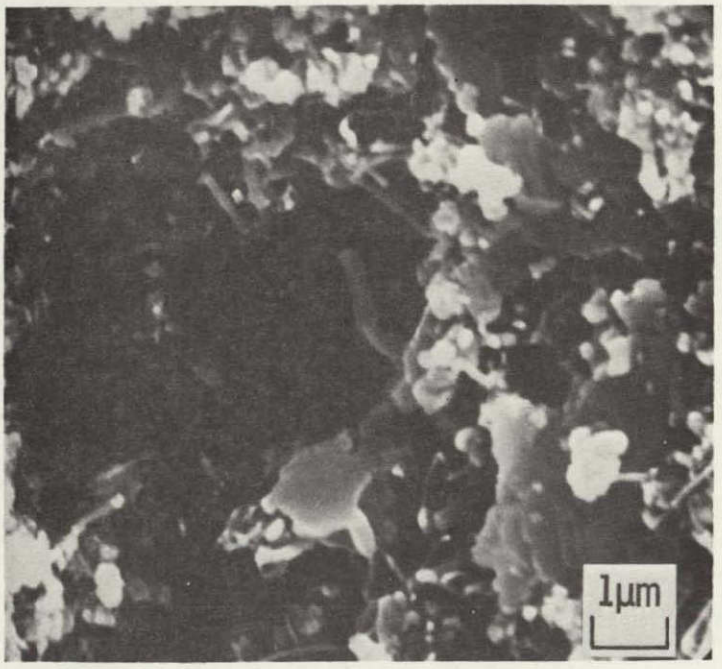

b. High purity Si + 1 percent Fe

Figure 29. SEM micrograph of fracture surface of Si_3N_4 nitrided in N_2, 4h, 1200°C

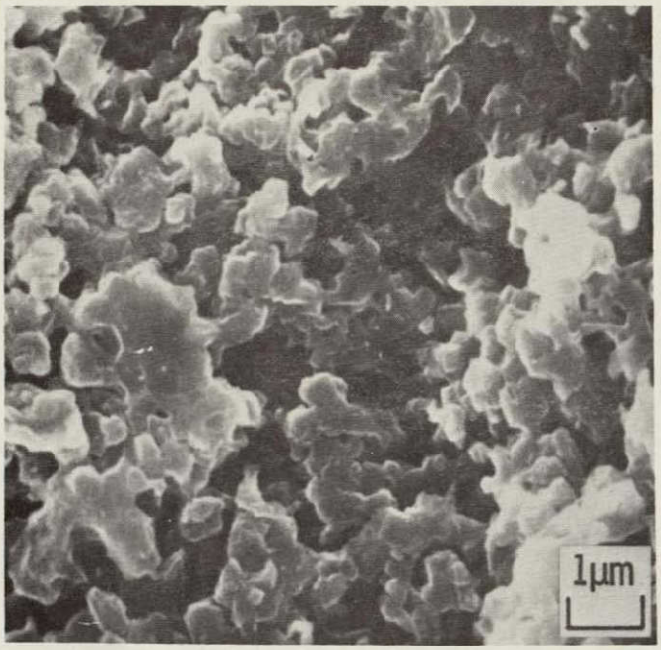

a. High purity Si

b. High purity Si + 1 percent Fe

Figure 30. SEM micrograph of fracture surface of Si_3N_4 nitrided in N_2/4 percent H_2, 4h, 1200°C

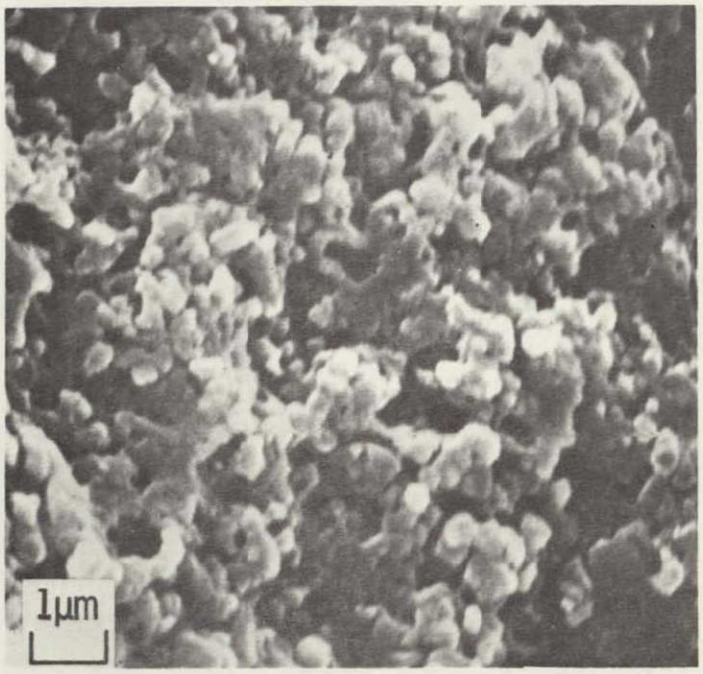

a. High purity Si

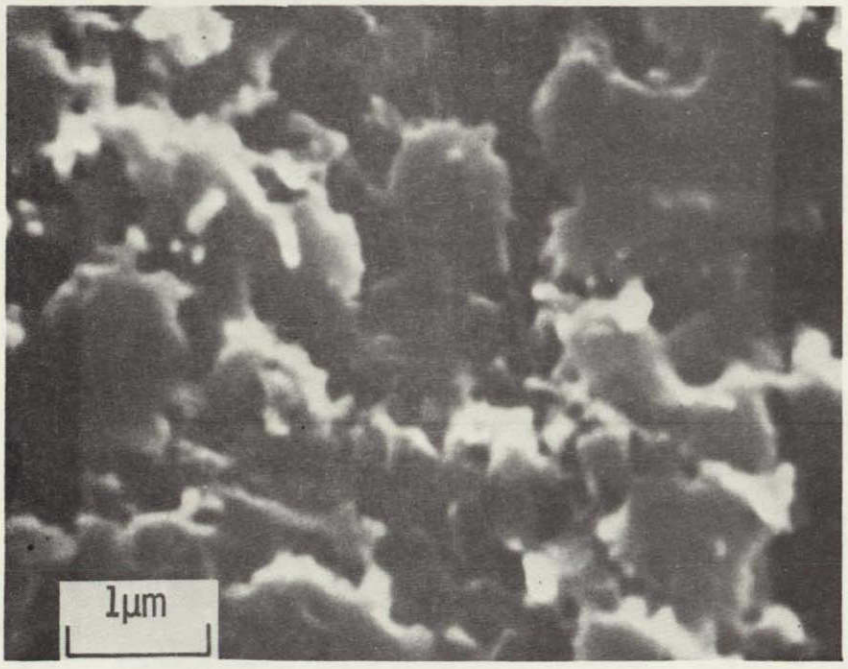

b. High purity Si + 1 percent Fe

Figure 31. SEM micrograph of fracture surface of Si_3N_4 nitrided in N_2, 4h, 1375^oC

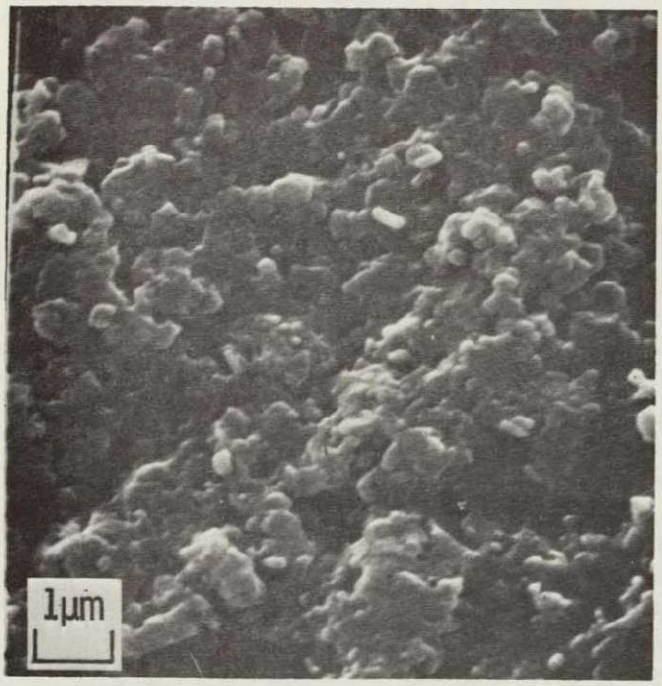

a. High purity Si

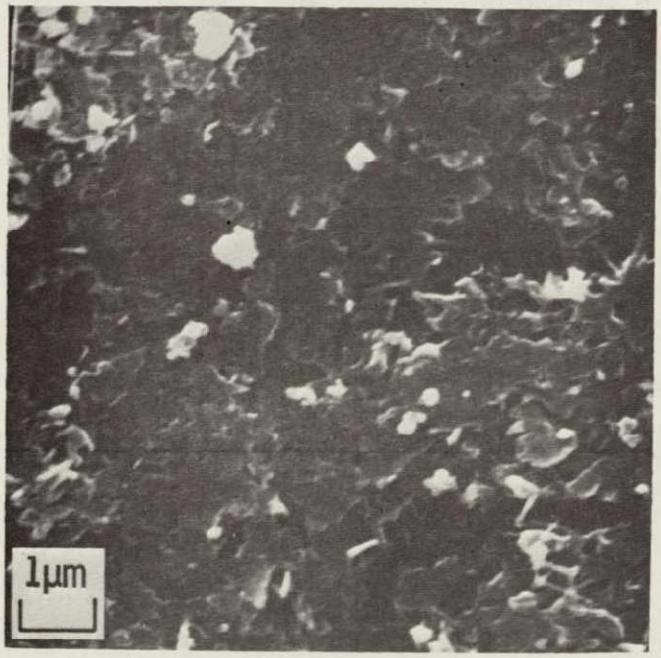

b. High purity Si + 1 percent Fe

Figure 32. SEM micrograph of fracture surface of Si_3N_4 nitrided in N_2/4 percent H_2, 4h, 1375°C

inhibiting complete nitridation. Whiskers and the mat structure are observed when Fe is added to the Si. Gribkov et al. (1972) suggested that α-Si_3N_4 whiskers grow in the presence of Fe or Al by a vapor-liquid-solid (VLS) mechanism. Atkinson et al. (1976) also noted whisker growth in tne presence of Fe, but not in pure Si, and suggested tnat such growth interfered with formation of coherent, nitride-inhibiting nitride film. However, whisker growth per se does not stop formation of such an inhibiting layer since such a layer is observed on single crystals and large particles that also have whiskers on them. Boyer and Moulson (1978) have also since rejected the proposal. Lindley et al. (1979) have attributed increased α-Si_3N_4 whisker mat development and increased RBSN strength to H_2. However, the powder they studied contained 0.87 percent Fe which apparently causes the initial formation of the whiskers.

Nitridation of Si Single Crystal Wafers

Formation of Si_3N_4 on the single crystal wafers nitrided near, but not in contact with, powder compacts was limited to a thin (< 10μm) surface layer. At the outer surface the nitride layer appears to be quite dense similar to that reported by Guthrie and Riley (1973). Pores as large as 8-10μm form at the nitride-silicon interface. Figure 33 is one example of this structure. Dalgleish,

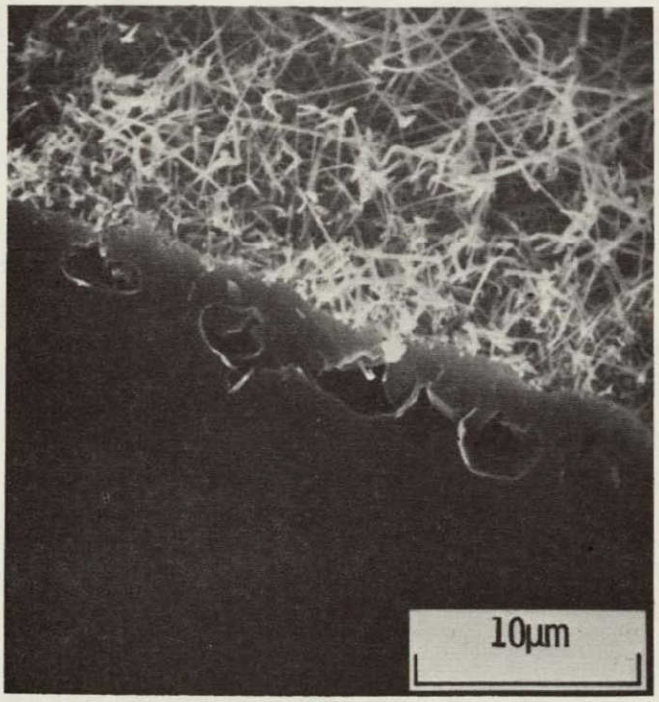

Figure 33. SEM micrograph of cross-section of nitrided {111} Si single crystal wafer with pores below surface Si_3N_4 layer. N_2, 1350°C, 24h

Jennings and Pratt (1981) reported the formation of similar structures following nitridation of Si single crystal wafers acid-cleaned in an effort to remove the SiO_2 layer. Their work showed differences in the shape of the subsurface pores depending on the crystallographic orientation of the nitrided Si substrate. They also found the thickness of the nitride layer and pore size and distribution to be related to nitridation temperature and the use of static or flowing N_2. They suggested that a nitride layer first covers the Si surface, followed by formation of the pores, perhaps by evaporation of Si through the nitride or vacancy coalescence.

In the present study a wafer with an acetone-iron slurry painted on it prior to nitridation, had many pores with channels open through the nitride layer (Figure 34). Energy dispersive X-ray analysis at the mouth of such pores (Figure 35) showed the presence of Fe. No Fe was found above closed pores.

Campos-Loriz, Howlett, Riley and Yusaf (1979) have proposed that the reaction rate of Si nitridation is controlled by the density of active surface sites. They suggested that these sites originate at flaws in the silica layer and then consist of channels in the Si_3N_4 through which Si vapor diffuses outward leaving the large pores at the Si/Si_3N_4 interface. Nitridation will then continue until the closure of these pores. Boyer et al. (1976) proposed the creation of localized flaws in the silica layer caused by

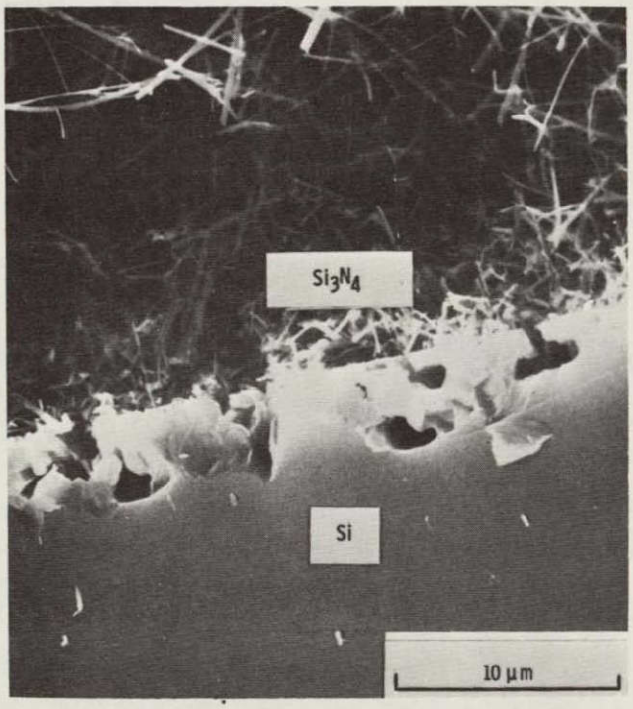

Figure 34. SEM micrograph of cross-section of nitrided {111} Si single crystal wafer with Fe on the surface showing open channels from pores through the surface Si_3N_4 layer. N_2, 1375°C, 4h

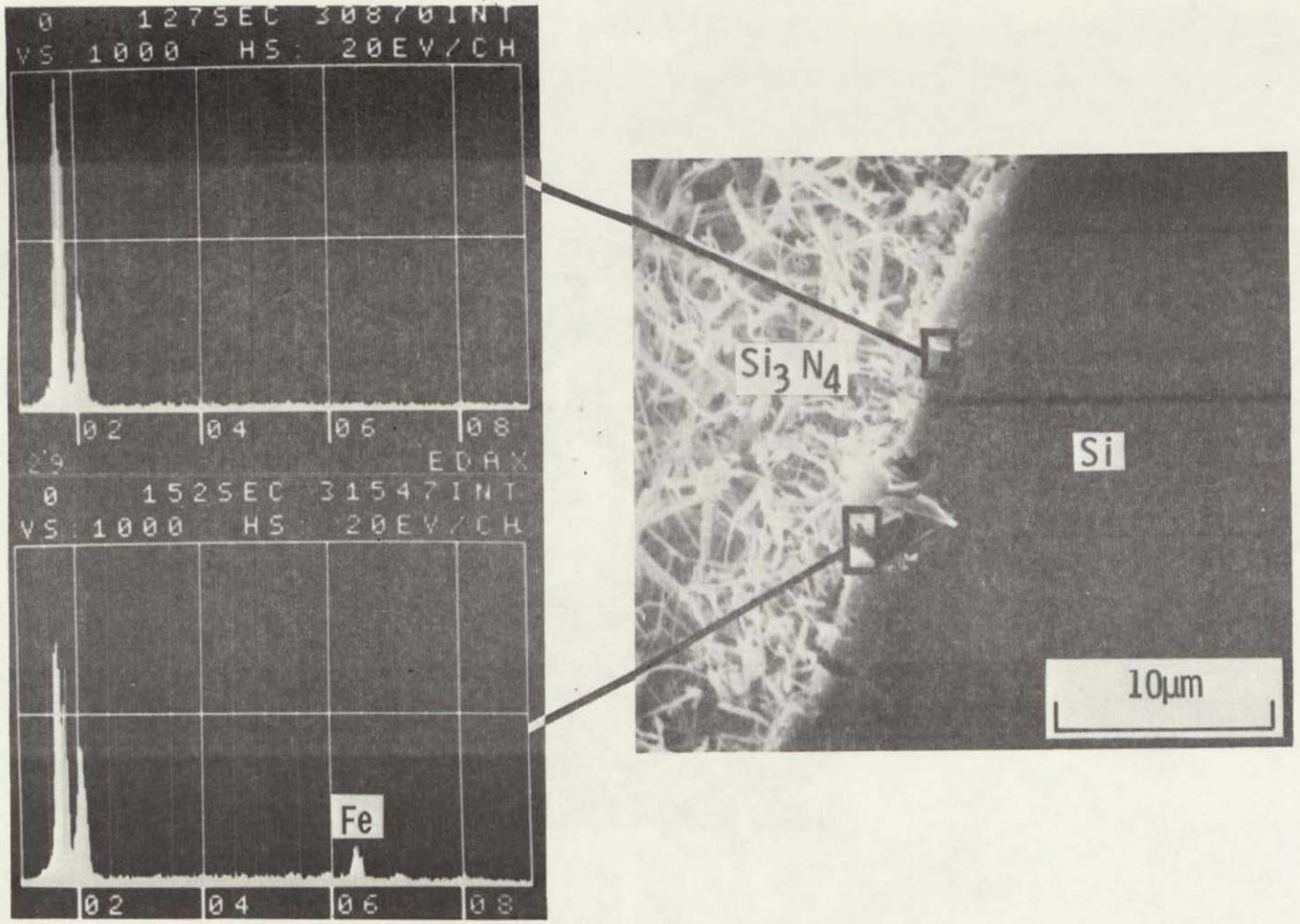

Figure 35. - Fe present at mouth of pores remaining open through Si_3N_4 layer (cross-sectional view) on (111) Si single crystal wafer nitrided in N_2 at 1375° C, 4h.

devitrification of the silica by Fe with further enlargement of the flaws by the reaction,

$$Si(s)+SiO_2(s) = 2SiO(g) \quad (6)$$

The photographic and x-ray evidence presented in Figure 35 suggests that the increased nitridation in the presence of Fe results, at least in part, from the presence of these Fe-initiated pore channels which allow access between N_2 and Si.

Most of the wafer surfaces, especially those nitrided at 1375^{o}C, have a layer of α-Si_3N_4 whiskers. These whiskers usually are cylindrical with an extremely high aspect ratio (Figure 36a). Some, however, grow instead as blades (Figure 36b).

Gribkov et al. (1972) studied Si_3N_4 whiskers grown on mullite from the reaction of Si and SiO_2 in a N_2/1 percent H_2 atmosphere. They suggested that these cylindrical whiskers were formed by a VLS mechanism involving a low melting Fe- or Al-Si composition that would leave a frozen droplet at the whisker tip. Such droplets were seen on a sample nitrided in N_2 at 1375^{o}C (Figure 37). Energy dispersive X-ray analysis indicated a high metallic element content, primarily Fe, in the droplet, but no Fe in the needle shaft indicating that the Si_3N_4 precipitated from the liquid onto the growing whiskers. The source of the Fe was uncertain, although an Fe-containing compact was also in the furnace.

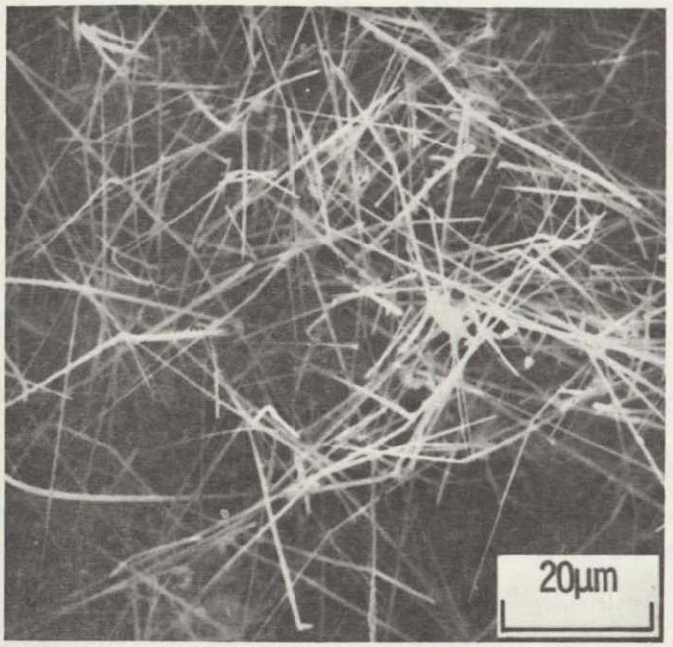

a. Cylindrical whiskers

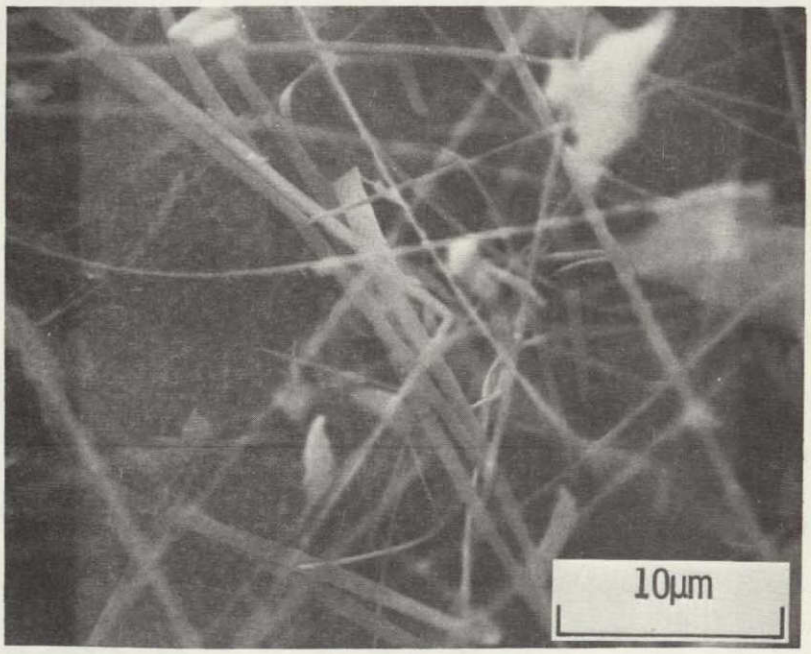

b. Blades

Figure 36. SEM micrographs of whisker growth on nitrided Si {111} wafers

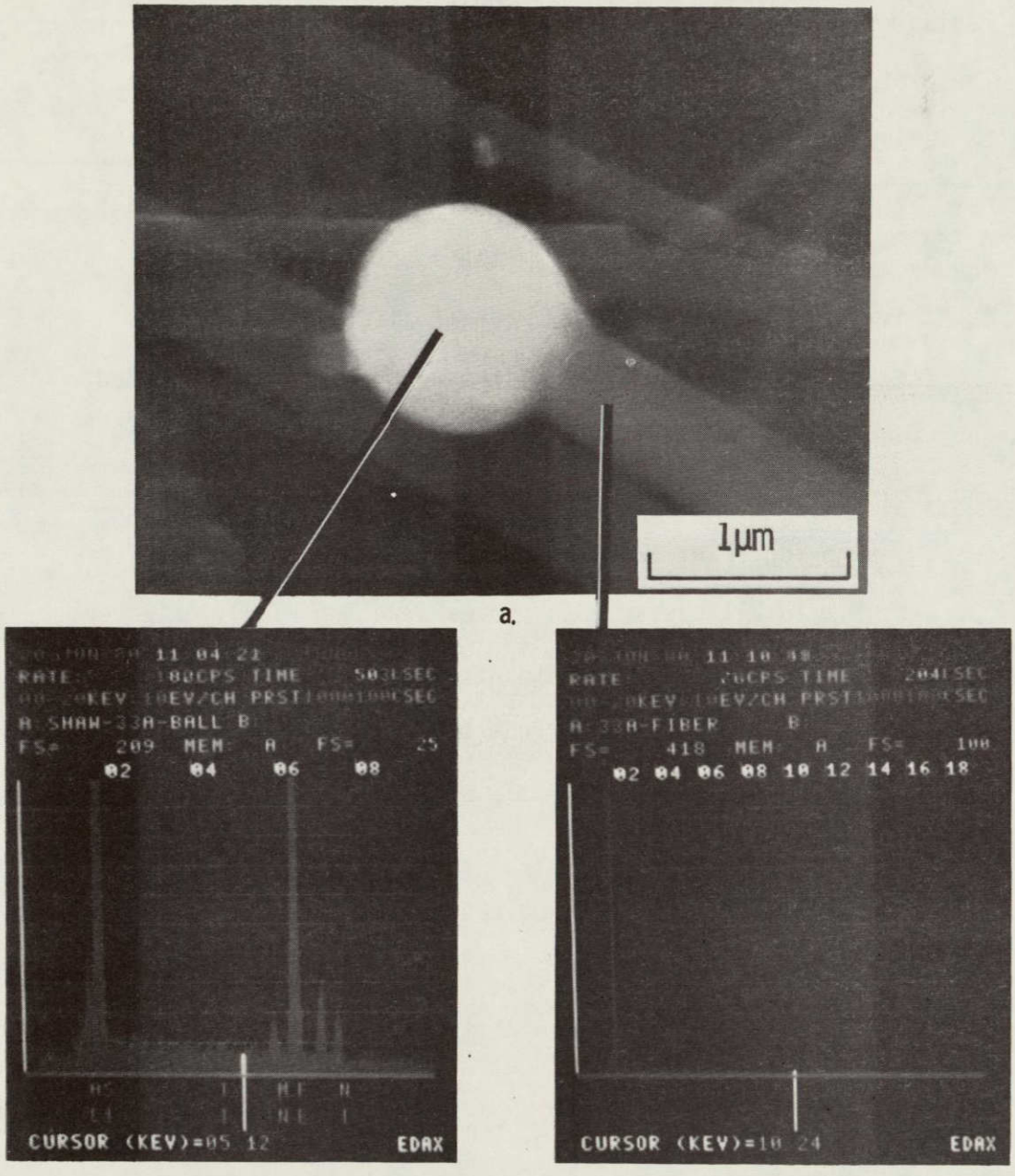

Figure 7 . - (a) SEM micrograph of droplet on end of α-Si_3N_4 whisker.
(b) X-ray indication of metallic elements in droplet.
(c) X-ray indication of no metallic elements in whisker shaft.

Gribkov et al. (1972) showed that α-Si_3N_4 crystallized in the form of blades from a liquid phase by an axial-screw-dislocation mechanism. Figure 36b shows a large number of these blades on a region of Si wafer that had been coated with Fe prior to nitriding. These blades were occasionally seen on other wafers.

Gribkov et al. (1972) showed that the presence Fe or Al was necessary for Si_3N_4 whisker growth. This study indicates that perhaps the amount of Fe controls the shape of the whiskers and mechanism of growth with blades being formed in high-Fe regions.

X-ray diffraction analysis of the wafer surfaces indicated formation of both α- and β-Si_3N_4 except on the wafer nitrided at 1200°C in N_2 which had only α-Si_3N_4. Only slight amounts of β-Si_3N_4 were formed at 1200°C in N_2/1 percent H_2 or N_2/4 percent H_2. In all cases, both phases were too highly oriented to allow calculation of relative amounts of each. At 1200°C the only significant β-Si_3N_4 peaks were from the $(20\bar{2}0)$ planes.

Crystallographic texture of the wafers is shown by an inverse pole figure in which the ratio of the relative intensity of the peak height is plotted against the angle between these planes and the $(20\bar{2}0)$ plane.

From the diffraction pattern of the wafer, values are determined for

$$R(hk\bar{i}l)=[I(hk\bar{i}l)/\ \Sigma hk\bar{i}l\ I(hk\bar{i}l)] \qquad (11)$$

where $I(hk\bar{i}l)$ is the diffraction peak intensity for the $(hk\bar{i}l)$ reflection. Similar values, R_o, were calculated from the ASTM standard powder patterns (1980). The ratio

$$R'(hk\bar{i}l) = R(hk\bar{i}l)/R_o(hk\bar{i}l) \quad (12)$$

is then plotted against Θ, the angle between $(hk\bar{i}l)$ and $(20\bar{2}0)$. For a randomly oriented sample, R' is unity for all Θ. Values of R' >1 indicate a preferred orientation.

The texture of β-Si_3N_4 formed at 1375°C with each level of H_2 is shown in Figure 38. Lines are drawn between the highest points at each angle. In N_2 only, there is a significant preferred orientation of the basal plane as had been observed by Guthrie and Riley (1973). The $(20\bar{2}0)$ are planes of N_2 atoms. The basal plane is made up of separated Si_3N_4 units. The $(20\bar{2}0)$ texture becomes greater with increasing H_2 content. Heckingbottom (1969) reported $(20\bar{2}0)$ preferred orientation during nitridation in HH_3 observed by low energy electron diffraction and attempted a detailed match between the substrate and the layer. (They referred to it as α-Si_3N_4, but the cell measurements used were for β-Si_3N_4.) The effort was only slightly successful for the (111) Si plane and not at all for the (311). They concluded (Heckingbottom and Wood 1973) that "formation and orientation of nitride nuclei are determined by the geometry of localized sites" with subsequent growth determined by intra-layer bonding.

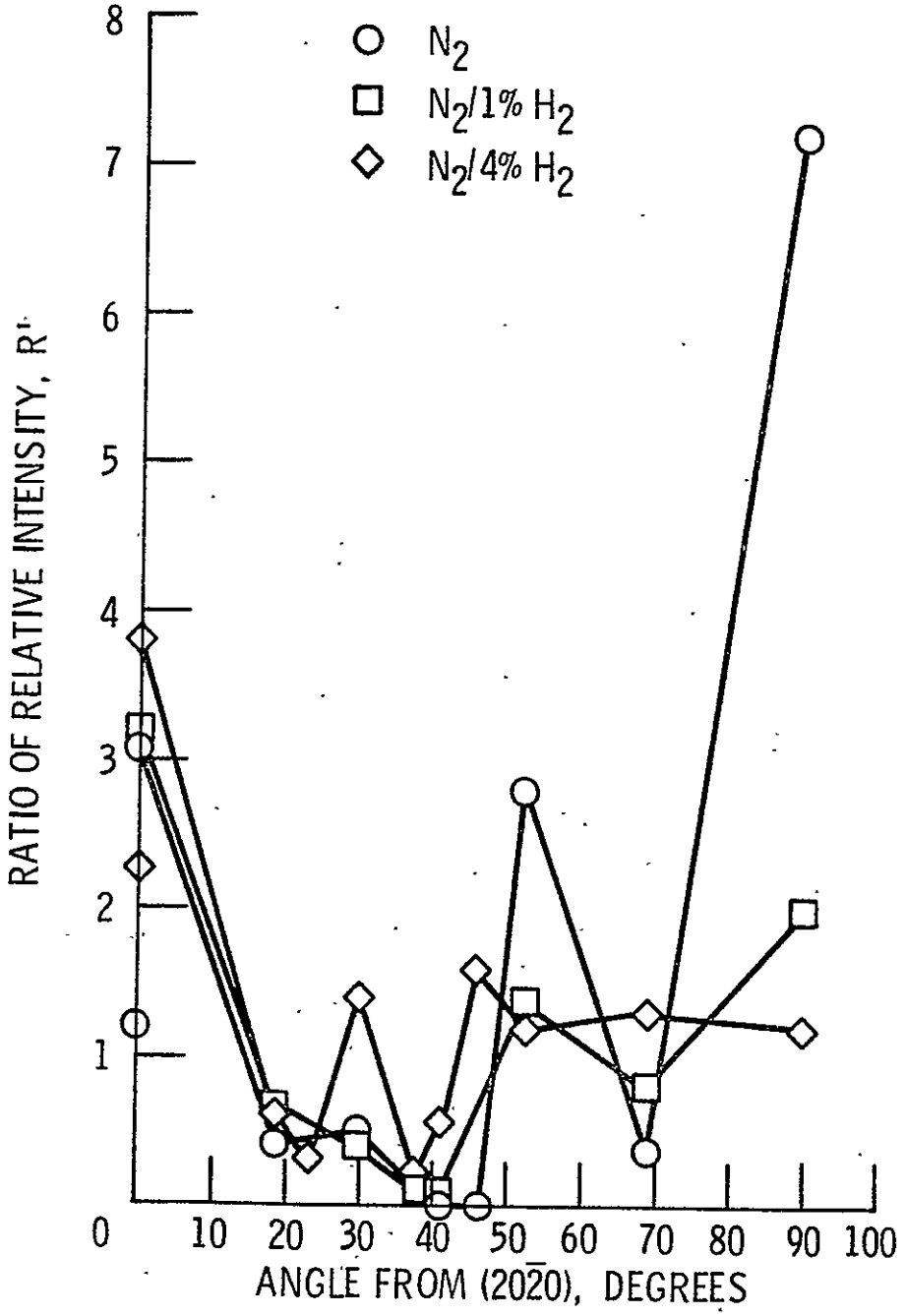

Figure 38. - Relative X-ray intensity vs. angle from (20$\bar{2}$0) plane for β-Si_3N_4 on (111) Si single crystal wafer nitrided at 1375° C, 4h.

The inverse pole figures for α-Si_3N_4 at 1200° and 1375°C are shown in Figures 39 and 40, respectively. At 1200°C in N_2 only, the basal plane is again the preferred orientation with the $(20\bar{2}0)$ orientation becoming more pronounced with increasing H_2 content. At 1375°C, three orientations, $(20\bar{2}0)$, $(10\bar{1}0)$ and (0002) have a similar degree of relative X-ray intensity which doesn't appear to have any particular relationship to H_2 content.

Both α-Si_3N_4 at low temperature and β-Si_3N_4 at high temperature appear to initially grow with the same preferred orientation that depends on H_2 content and then, at least in the case of α, continue growth in a variety of directions.

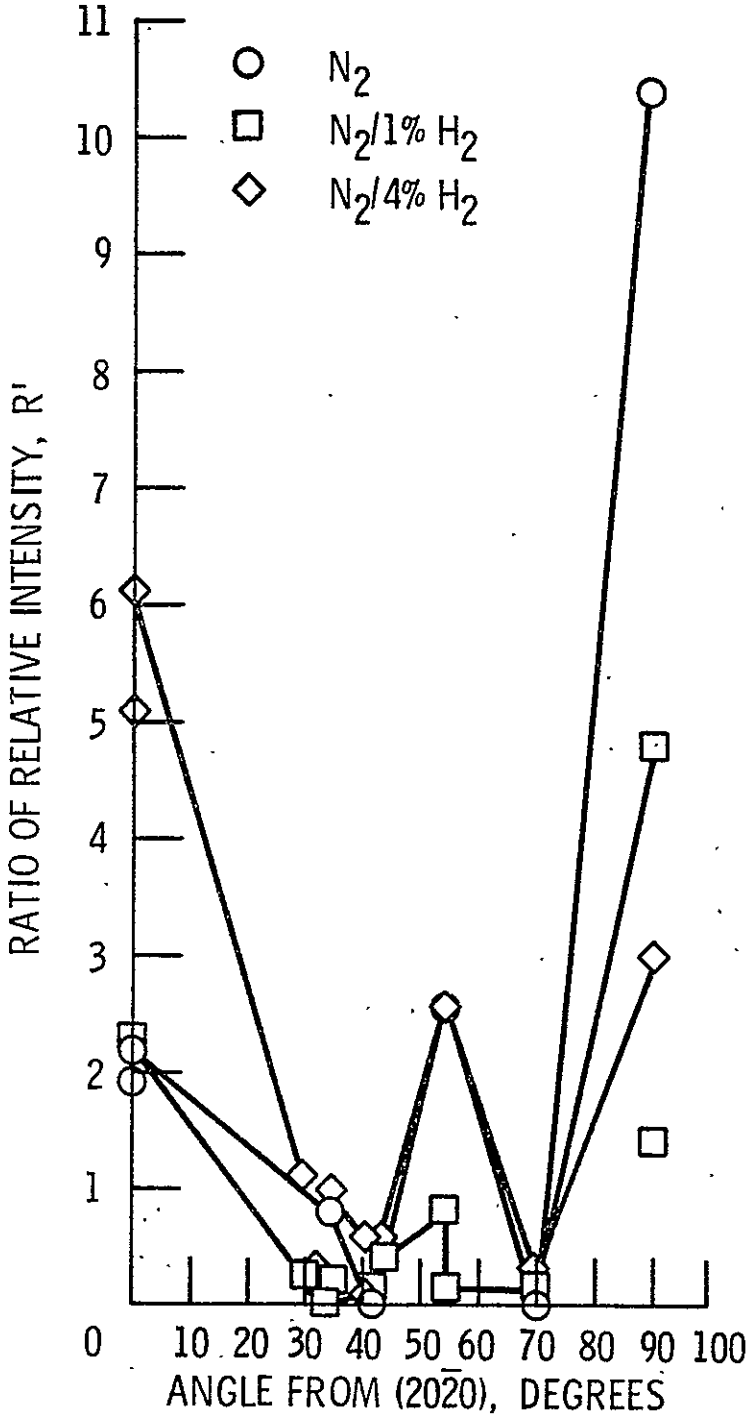

Figure 39. - Relative X-ray intensity vs. angle from (20$\bar{2}$0) plane for α-Si_3N_4 on (111) Si single crystal wafer nitrided at 1200° C, 4h.

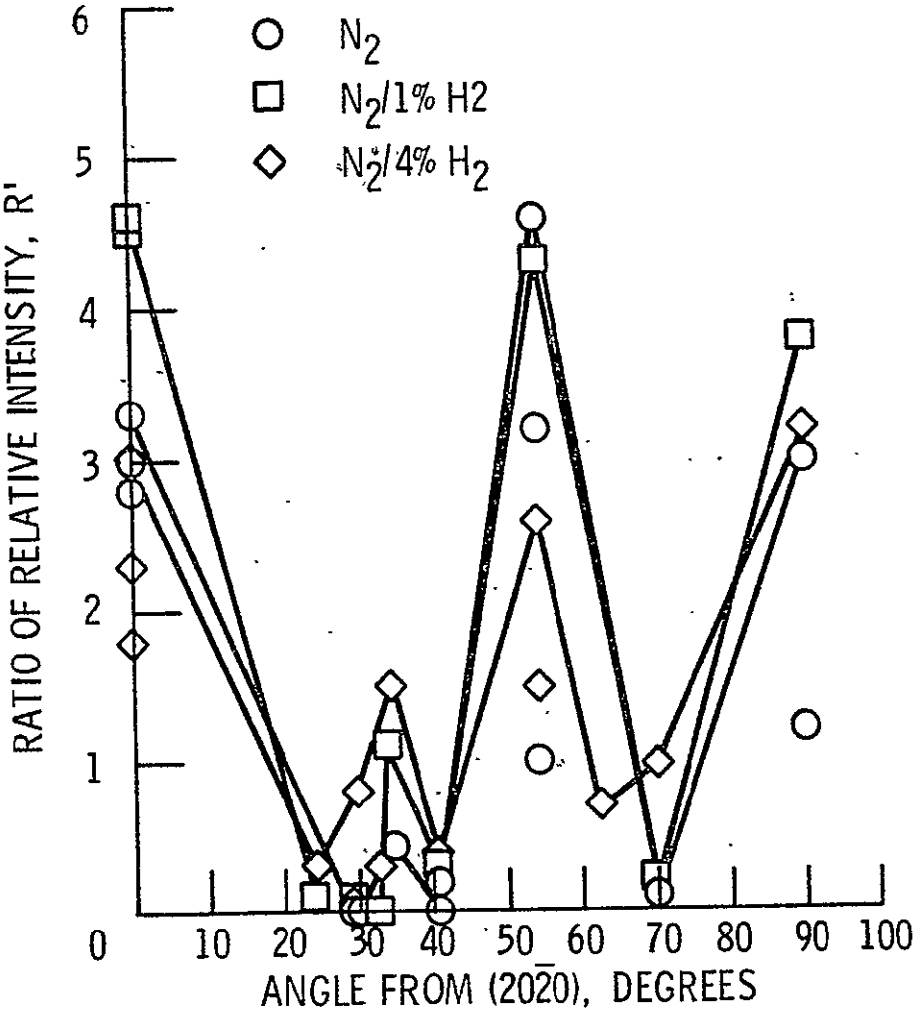

Figure 40. - Relative X-ray intensity vs. angle from (20$\bar{2}$0) plane for α-Si_3N_4 on (111) Si single crystal wafer nitrided at 1375^0 C, 4h.

V. CONCLUSIONS

Several simple chemical reactions have been suggested to contribute to the process, and the possible importance of gaseous species such as SiO, O_2 and H_2O have been considered. The thermodynamic calculations made in this study showed that in the presence of H_2, both NH_3 and SiH_4 are formed in significant amounts. They may contribute to the increased nitridation and, especially, α-Si_3N_4 formation attributed to H_2 since NH_3 and SiH_4 can react in the vapor phase to form α-Si_3N_4.

It had been previously reported that Si_3N_4 whiskers were not present on high purity Si, but that they did form in the presence of Fe. This was confirmed in this study, suggesting that the increased α-Si_3N_4 whisker formation attributed to H_2 occurs only after initiation of whisker growth by Fe.

Fe is known to increase both the rate and degree of nitridation. One explanation for these effects is the initiation by Fe of localized flaws in the SiO_2 layer and formation of open channels through the nitride layer on the Si single crystal surface to pores beneath the layer. These channels provide continuing access of N_2 to the Si throughout nitridation.

The orientation of both α- and β-Si_3N_4 on the Si single crystal wafer appears to change from basal planes, // to Si {111} to

$(20\bar{2}0)$ when H_2 is added to the N_2. This change in a preference of orientation may be a factor in the increased nitridation observed in N_2/H_2 atmospheres.

Hydrogen appears to in some manner suppress surface diffusion of Si resulting in much less particle growth than in He. This may involve the removal of the SiO_2 layer which may act as a fast transport path or the physi-or chemisorption of H_2 on the particles.

Other observations from either the thermodynamic calculations or experiment are that:

Hydrogen

- enhances removal of $SiO_2(s)$ from Si
- when $SiO_2(s)$ is present
  - increases SiO(g), Si(g)
  - decreases $O_2(g)$
  - allows formation of $Si_3N_4(s)$
- has no effect on these species when SiO_2 is removed
- keeps Si particle size small during sintering
- increases degree of nitridation

Iron

- promotes full nitridation at 1375°

It is proposed that nitridation is initially enhanced by H_2-assisted removal of the SiO_2 layer from the Si and formation of Si-containing vapor species and NH_3 at or somewhat below

1200°C. Localized flaws are initiated in the SiO_2 by Fe. Fe induces the formation of Si_3N_4 whiskers, the growth of which is then enhanced by H_2. Additional α-Si_3N_4 is formed by the vapor phase reaction of NH_3 and SiH_4. Effects of H_2 diminish as the SiO_2 is removed. Once the SiO_2 is effectively disrupted and nitridation is occuring, Fe acts to maintain open channels through the nitride forming on the Si particles, allowing free access of N_2 to the underlying Si until nitridation is complete by both vapor phase and surface reactions.

VI. SUGGESTIONS FOR FUTURE WORK

The mechanisms of formation of Si_3N_4 have not been determined. There are many questions that could be addressed with transmission electron microscopy and electron diffraction, preferably under conditions allowing observation of Si_3N_4 formation in situ. How do the α- and β-phases nucleate? Which phase forms the Si_3N_4 layer on the Si particle or wafer? Do the whiskers grow from the Si or the Si_3N_4 layer? What are the conditions for growth of different Si_3N_4 morphologies? What is mechanism of formation of the open channels through the nitride in the presence of Fe? What is the effect of the presence or absence of the SiO_2 layer on the transport mechanism and sintering behavior of Si?

Other questions of interest are: Is there another form of Fe that could be added to high purity Si to enhance nitridation without the usual inhomogenities? Will something other than Fe work as well and not create inhomogenities in the presence of H_2? What other Si or atmospheric impurities may be having a significant effect on either degree of nitridation or microstructure?

VII. REFERENCES

1. Arundale, P.; and Moulson, A. J.: Microstructural Changes During the Argon-Sintering of Silicon Powder Compacts. J. Mater. Sci., vol. 12, no. 10, Oct. 1977, pp. 2138-2140.

2. Atkinson, A.; Moulson, A. J.,; and Roberts, E. W.: Nitridation of High-Purity Silicon," J. Am. Ceram. Soc., vol. 59, no. 7-8, July-Aug. 1976, pp. 285-289.

3. Atkinson, A.; and Moulson, A. J.: Some Imporant Variables Affecting the Course of the Reaction Between Silicon Powder and Nitrogen. Science of Ceramics, Gerald H. Stewart, editor. Vol. 8 Academic Press for the British Ceramic Society, 1976, pp. 111-121.

4. Blegen, Karl: Equilibria and Kinetics in the Systems Si-N and Si-N-O, Special Ceramics, P. Popper, editor. Vol. 6. British Ceramic Research Association, Stake-on-Trent, 1975, pp. 223-244.

5. Boyer, S. M.; Sang, D.; and Moulson, A. J.: The Effects of Iron on the Nitridation of Silicon. Nitrogen Ceramics, F. L. Riley, editor. Noordhoff (Leyden), 1977, pp. 297-312.

6. Boyer, S. M.; and Moulson, A. J.: A Mechanism for the Nitridation of Fe-Contaminated Silicon. J. Mater. Sci., vol. 13, no. 8, Aug. 1978, pp. 1637-1646.

7. Campos-Loriz, D.; et al.: Fluoride Accelerated Nitridation of Silicon. J. Mater. Sci., vol. 14, no. 10, Oct. 1979, pp. 2325-2334.

8. Campos-Loriz, D.; and Riley, F. L.: Factors Affecting the Formation of the α- and β-phases of Silicon Nitride in the Nitridation of Silicon Powders, Science of Ceramics, K. J. DeVries, editor. Vol. 9. Academic Press for the British Ceramic Society, 1977, pp. 38-45.

9. Campos-Loriz, D.; and Riley, F. L.: Factors Affecting the Formation of the α- and β-phases of Silicon Nitride. J. Mater. Sci., vol. 13, no. 5, May 1978, pp. 1125-1127.

10. Cartz, L.; and Jorgensen, J. D.: The High-Pressure Behavior of α-quartz, Oxynitride, Nitride Structures. J. Appl. Phys., vol. 52, no. 1, Jan. 1981, pp. 236-244.

11. Chen, Y. J: Kinetics and Microstructure Studies of Silicon Reacted with H_2/N_2 Gas Mixtures. M. S. Thesis, Cleveland State University, 1980.

12. B. J. Dalgleish, H. M. Jennings and P. L. Pratt, "The Formation of Nitrides on the Pure Silicon Surfaces," to be published in Proc. Brit. Ceram. Soc. 30 (1981).

13. Dawson, W. M.; Arundale, P.; and Moulson, A. J.: Development and Control of Microstructure in Reaction Bonded Silicon Nitride. Science of Ceramics, K. J. deVries, editor, Vol. 9 Academic Press for the British Ceramic Society, 1977, pp. 111-118.

14. Dawson, W. M.; and Moulson, A. J.: The Combined Effects of Fe and H_2 on the Kinetics of Silicon Nitridation. J. Mater. Sci., vol. 13, no. 10, Oct. 1978, pp. 2289-2290.

15. Dervisbegovic, H.; and Riley, F. L.: The Influence of Iron and Hydrogen in the Nitridation of Silicon. J. Mater. Sci., vol. 14, no. 5, May 1979, pp. 1265-1268.

16. Elias, D. P.; Jones, B. F.; and Lindley, M. W.: The Formation of the α- β- Phases in Reaction Sintered Silicon Nitride and Their Influence on Strength. Powder Metall. Int., vol. 8, no. 4, Nov. 1976, pp. 162-165.

17. Evans, A. G.; and Sharp, J. V.: Microstructural Studies on Silicon Nitride. J. Mater. Sci., vol. 6, no. 10, Oct. 1971, pp. 1292-1302.

18. Forgeng, W. D.; and Decker, B. F.: Nitrides of Silicon," Trans. Am. Inst. Min. Metall. Pet. Eng., vol. 212, no. 6, June 1958, pp. 343-348.

19. Frost, Arthur A.; and Pearson, Ralph G.: Kinetics and Mechanism: A Study of Homogeneous Chemical Reactions. Wiley, 1953.

20. Gazzara, Charles P.; and Messier, Donald R.: Determination of Phase Content of Si_3N_4 by X-ray Diffraction Analysis, Am. Ceram. Soc. Bull., vol. 56, no. 9, Sept. 1977, pp. 777-780.

21. T. K. Glasgow, Unpublished research.

22. Gordon, S.; and McBride, B. J.: Computer Program for Calculation of Complex Chemical Equilibrium Compositions, Rocket Performance, Incident and Reflected Shocks, and Chapman-Jouquet Detonations. NASA SP-273 Rev. 1976.

23. Greskovich, C.; and Rosolowski, J. H.: Sintering of Covalent Solids. J. Am. Ceram. Soc., vol. 59, no. 7-8, July-Aug. 1976, pp. 336-343.

24. Gribkov, V. N.; et al.: Growth Mechanisms of Silicon Nitride Whiskers. Sov. Phys.-Crystallogr. (Engl Transl.), vol. 16, no. 5, Mar.-April 1972, pp. 852-854.

25. Grieveson, P.; Jack, K. H.; and Wild, S.: The Crystal Structures of Alpha and Beta Silicon and Germanium Nitrides. Special Ceramics, P. Popper, editor. Vol. 4. British Ceramic Research Association, Stoke-on-Trent, 1968, pp. 237-238.

26. Guthrie, R. B.; and Riley, F. L.: The Nitridation of Single-Crystal Silicon. Ceramics for Turbines and Other High-Temperature Engineering Applications; Proceedings British Ceramic Society, no. 22, D. J. Godfrey, ed. British Ceramic Society, Stoke-on-Trent, 1973, pp. 275-280.

27. Guthrie, R. B.; and Riley, F. L.: Effect of Oxide Impurities on the Nitridation of High Purity Silicon. J. Mater. Sci., vol. 9, no. 8, Aug. 1974, pp. 1363-1365.

28. Hardie, D.; and Jack, K. H.: Crystal Structures of Silicon Nitride. Nature (London), vol. 180, Aug. 17, 1957, pp. 332-333.

29. Halliwell, M. A. G.; and Heckingbottom, R.: Direct Nitridation of the Si (111) Surface - A Low Energy Electron Diffraction Study, October 1967-December 1968. Rept.-61, General Post Office, London, 1968.

30. Heckingbottom, R.; and Wood, P. R.: A Study of the Nitridation of Silicon Surfaces by Low-Energy Electron Diffraction and Auger Electron Spectroscopy. Surf. Sci., vol. 36, 1973, pp. 594-605.

31. Hendry, A.: Thermodynamics of Silicon Nitride and Oxynitride. Nitrogen Ceramics, F. L. Riley, editor. Noordhoff (Leyden), pp. 183-185.

32. Heinrich, J.: The Effect of Preparation Conditions on the Structure and Mechanical Properties of Reaction-Sintered Silicon Nitride. NASA TM-75797, 1980.

33. Stull, D. R.; et al.: JANAF Thermochemical Tables. Second ed. NSRDS-NBS-37, Dow Chemical Co., 1971.

34. Jones, B. F.; and Lindley, M. W.: The Influence of Hydrogen in the Nitriding Gas on the Strength of Reaction Sintered Silicon Nitride. J. Mater. Sci., vol. 11, no. 10, Oct. 1976, pp. 1969-1971.

35. Kamchatka, M. I.; and Ormont, B. F.: Kinetics of the Nitridation of Silicon by Ammonia at High Temperatures. Russ. J. Phys. Chem. (Engl. Transl.), vol. 45, no. 9, Sept. 1971, pp. 1246-1249.

36. Kohatsu, I.; and McCauley, James W.: Re-examination of the Crystal Structure of α-Si_3N_4. Mater. Res. Bull., vol. 9, no. 7, July 1974, pp. 917-920.

37. Lin, Sin-Shong: Mass Spectrometric Studies of the Nitridation of Silicon. J. Am. Ceram. Soc., vol. 58, no. 7-8, July-Aug. 1975, pp. 271-273.

38. Lin, Sin-Shong: Comparative Studies of Metal Additives on the Nitridation of Silicon. J. Am. Ceram. Soc., vol. 60, no. 1-2, Jan.-Feb. 1977, pp. 78-81.

39. Lindley, M. W.; et al.: The Influence of Hydrogen in the Nitriding Gas on the Strength, Structure and Composition of Reaction-Sintered Silicon Nitride. J. Mater. Sci., vol. 14, no. 1, Jan. 1979, pp. 70-85.

40. Longland, P.; and Moulson, A. J.: The Growth of α- and β-Si_3N_4 Accompanying the Nitriding of Silicon Powder Compacts. J. Mater. Sci., vol. 13, no. 10, Oct. 1978, pp. 2279-2280.

41. Makowiecki, D. M.; and Holt, J. B.: Surface Self-Diffusion of Germanium and Silicon," Sintering Processes, G. C. Kuczynski, editor, Materials Science Research, Vol. 13, Plenum Press, 1980, pp. 279-288.

42. Mangels, John A.: Effect of H_2-N_2 Nitriding Atmospheres on the Properties of Reaction-Sintered Si_3N_4. J. Am. Ceram. Soc., vol. 58, no. 7-8, July-Aug. 1975, pp. 354-355.

43. Messier, Donald R.; and Wong, Philip: Kinetics of Nitridation of Si Powder Compacts. J. Am. Ceram. Soc., vol. 55, no. 9, Sept. 1973, pp. 480-485.

44. Mitomo, M.: Effect of Fe and Al Additions on Nitridation of Silicon. J. of Mater. Sci., vol. 12, no. 2, Feb. 1977, pp. 273-276.

45. P. E. D. Morgan: The α/β-Si_3N_4 Question," J. Mater. Sci., vol. 15, no. 3, Mar. 1980, pp. 791-793.

46. Moulson, A. J.: Reaction-Bonded Silicon Nitride: Its Formation and Properties. J. Mater. Sci., vol. 14, no. 5, May 1979, pp. 1017-1051.

47. Parr, N. L.; Martin, G. F.; and May, E. R. W.: Preparation, Microstructure, and Mechanical Properties of Silicon Nitride," Special Ceramics, P. Popper, editor. Academic Press, 1960, pp. 102-135.

48. Parr, N. L.; and May, E. R. W.: The Technology and Engineering Applications of Reaction-Bonded Si_3N_4," Proc. Br. Ceram. Soc., vol. 7, 1967, pp. 81-93.

49. Pehlke, R. D.; and Elliott, J. F.: High-Temperature Thermodynamics of the Silicon, Nitrogen, Silicon-Nitride System," Trans. Am. Inst. Min. Metall. Pet. Eng., vol. 215, Oct. 1959, pp. 781-785.

50. Powder Diffraction File. American Society for Testing and Materials, 1980.

51. Priest, H. F.; et al.: Oxygen Content of Alpha Silicon Nitride. J. Am. Ceram. Soc., vol. 56, no. 7, July 1973, pp. 395.

52. Ruddlesden, S. N.; and Popper, P.: On the Crystal Structures of the Nitrides of Silicon and Germanium. Acta. Crystallogr., vol. 11, 1958, pp. 465-468.

53. Shaw, N. J.; and Glasgow, T. K.: Formation of Porous Surface Layers in Reaction Bonded Silicon Nitride During Processing. NASA TM-81493, 1979.

54. Thompson, D. S.; and Pratt, P. L.: The Structure of Silicon Nitride. Science of Ceramics, G. H. Stewart, editor. Vol. 3. Academic Press for the British Ceramic Society, 1967, pp. 33-51.

55. G. E. Welsch, H. J. Moller, and A. H. Heuer, "Grain Growth in Sintered Polycrystalline Silicon," unpublished report to Sola Energy Research Institute, 1980.

56. G. E. Welsch, H. J. Moller, and A. H. Heuer, "Grain Growth in Sintered Silicon," unpublished report to Solar Energy Research Institute, 1981.

57. Wild, S.; Grieveson, P.; and Jack, K. H.: The Crystal Structures of Alpha and Beta Silicon and Germanium Nitrides. Special Ceramics, P. Popper, editor. Vol. 5. British Ceramic Research Association, Stoke-on-Trent, 1972, pp. 385-395.

58. Zelenik, Frank J.; and Gordon, S.: Calculation of Complex Chemical Equilibria," Ind. Eng. Chem., vol. 60, no. 6, June 1968, pp. 27-57.

1. Report No	2 Government Accession No	3. Recipient's Catalog No
NASA TM-82722		

4 Title and Subtitle	5. Report Date
NITRIDATION OF SILICON	October 1981
	6. Performing Organization Code 505-33-12

7. Author(s)	8. Performing Organization Report No
Nancy J. Shaw	E-921
	10. Work Unit No

9 Performing Organization Name and Address	11. Contract or Grant No.
National Aeronautics and Space Administration Lewis Research Center Cleveland, Ohio 44135	

12 Sponsoring Agency Name and Address	13. Type of Report and Period Covered
National Aeronautics and Space Administration Washington, D.C. 20546	Technical Memorandum
	14. Sponsoring Agency Code

15 Supplementary Notes

Report was submitted as a thesis in partial fulfillment of the requirements for the degree Master of Science to Case Western Reserve University, Cleveland, Ohio in August 1981.

16 Abstract

Silicon powders with three levels of impurities, principally Fe, were sintered in He or H_2. Non-densifying mechanisms of material transport were dominant in all cases. High purity Si showed coarsening in He while particle growth was suppressed in H_2. Lower purity powder coarsened in both He and H_2. The same three Si powders and Si {111} single crystal wafers were nitrided in both N_2 and N_2/H_2 atmospheres. H_2 increased the degree of nitridation of all three powders and the α/β ratio of the lower purity powder. Si_3N_4 whiskers and open channels through the surface nitride layer were observed in the presence of Fe, correlating with the nitridation-enhancing effects of Fe. Thermodynamic calculations showed that when SiO_2 is present on the Si, addition of H_2 to the nitriding atmosphere decreases the amount of SiO_2 and increases the partial pressure of Si-containing vapor species, e.g. Si and SiO. Large amounts of NH_3 and SiH_4 were also predicted to form.

17. Key Words (Suggested by Author(s))	18. Distribution Statement
Reaction bonded silicon nitride; Nitridation; Effects of H_2 and Fe on nitridation; Sintering of Si; Si single crystal nitridation	Unclassified - unlimited STAR Category 27

19 Security Classif. (of this report)	20. Security Classif. (of this page)	21. No of Pages	22 Price*
Unclassified	Unclassified		

* For sale by the National Technical Information Service, Springfield, Virginia 22161

National Aeronautics and Space Administration

Washington, D.C.
20546

Official Business
Penalty for Private Use, $300

SPECIAL FOURTH CLASS MAIL
BOOK

Postage and Fees Paid
National Aeronautics and
Space Administration
NASA-451

POSTMASTFR: If Undeliverable (Section 158
Postal Manual) Do Not Return